

## **General Disclaimer**

### **One or more of the Following Statements may affect this Document**

- This document has been reproduced from the best copy furnished by the organizational source. It is being released in the interest of making available as much information as possible.
- This document may contain data, which exceeds the sheet parameters. It was furnished in this condition by the organizational source and is the best copy available.
- This document may contain tone-on-tone or color graphs, charts and/or pictures, which have been reproduced in black and white.
- This document is paginated as submitted by the original source.
- Portions of this document are not fully legible due to the historical nature of some of the material. However, it is the best reproduction available from the original submission.

MICROELECTRONIC BIOINSTRUMENTATION  
SYSTEMS - NDR-36-027-053

Proposal and Progress Report  
July 18, 1975

(NASA-CR-143088) MICROELECTRONIC  
BIOINSTRUMENTATION SYSTEMS Annual Report,  
Jul. 1974 - Jun. 1975 (Case Western Reserve  
Univ.) 69 p HC \$4.25

CSSL 06B

N75-27339

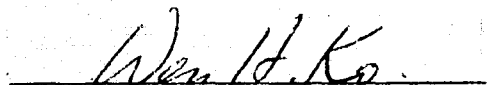
Unclas  
28047

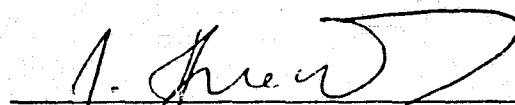
G3/35

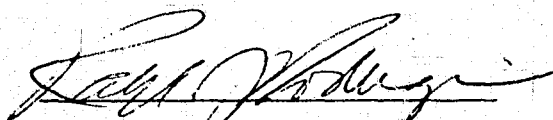


MICROELECTRONIC BIOINSTRUMENTATION SYSTEMS

Submitted to  
AMES RESEARCH CENTER  
NATIONAL AERONAUTICS and SPACE ADMINISTRATION

  
Wen H. Ko, Ph. D.  
Principal Investigator  
Director -  
Engineering Design Center

  
Jaroslav Hynecek, Ph.D.  
Co-Principal Investigator  
Chief Engineer  
Engineering Design Center

  
Ralph J. Rodriguez  
Research Administration  
Assistant Director

ENGINEERING DESIGN CENTER  
Case Institute of Technology  
Case Western Reserve University  
Cleveland, Ohio 44106

## TABLE OF CONTENTS

Budget .....	1
Proposal.....	2
RF Powered Single Channel ECG Telemetry System.....	2
Development of the RF Powered Cage and the Detecting Circuitry.....	2
Single Channel Orientation Independent Powering.....	3
Three Channel RF Powered Telemetry System.....	3
Annual Report	
I. Progress Reports	
Single Frequency RF Powering.....	5
RF Powered Cage Design and Considerations.....	12
Ingestible Telemetry System.....	25
M-5A Pulse Frequency PFM Modulator.....	44
Demodulator for Three Channel RF Powered Telemetry System.....	50
II. Publications and Theses .....	64



## PROPOSED BUDGET SEPTEMBER 1, 1975 - AUGUST 31, 1976

## NASA GRANT - MICROELECTRONIC BIOINSTRUMENTATION SYSTEMS

## PERSONNEL

Wen H. Ko	10%	\$4,000
Robert Collin	10%	2,965
Jaroslav Hyncek-Chief Engineer	30%	6,140
Louis Greene - Engineer	15%	1,885
Louis Sagys - Technician	15%	1,885
A. Kou - Graduate Assistant	100%	6,780
C. Fung - Graduate Assistant	100%	6,780
Machinists	15%	<u>1,900</u>

Total Direct Personnel Cost	\$ 32,335
-----------------------------	-----------

Fringe Benefits---15.5%	5,012
-------------------------	-------

Indirect Costs---65%	<u>21,018</u>
----------------------	---------------

TOTAL PERSONNEL & INDIRECT COST	\$58,365
---------------------------------	----------

## EQUIPMENT (to improve facilities for telemetry system research &amp; development)

Astro Receiver for Telemetry System Development	\$ 2,500	
RF Oscillator and 30 Watt Power Amp.	1,500	
Sealing Jig for Laser Seal of Glass Caps.	<u>1,000</u>	
Total Equipment		\$5,000

## SUPPLIES

Chemical, Materials and Supplies for Semiconductor Process	\$ 3,000	
Semiconductors and Integrated Circuits	3,000	
General Electronics Supplies	2,000	
Packaging Materials	1,000	
Photographic and Office Supplies	<u>1,000</u>	
Total Supplies		\$10,000

TRAVEL, COMMUNICATIONS AND PUBLICATIONS	\$ 2,000
---	----------

Total	<u>\$17,000</u>
-------	-----------------

TOTAL PROJECT COST	<u>\$75,365</u>
--------------------	-----------------

## MICROELECTRONICS BIOINSTRUMENTATION SYSTEMS PROPOSAL

For the continuation of Research Grant NDR-36-027-053, we propose to perform the following work.

### 1. RF Powered Single Channel ECG Telemetry System

The single channel ECG system, delivered to Dr. H.L. Stone for evaluation, will be duplicated and several more transmitters (implants) will be built which will be compatible with existing RF powering units. They will be implanted in monkeys and dogs for base line data collection, to test implant procedures and to establish device reliability.

These units will basically be the same as the units previously built, with minor modifications and improvements of the sensitivity and noise. Some changes and improvements will also be made on the packaging of the units. Sealed glass packages may be used when the laser sealing facility is in operation.

### 2. Development of the RF Powered Cage and the Detecting Circuitry

We propose to build a cylindrically shaped cage which will be excited by the RF field from axially placed conductors in the center of the cage. Preliminary experiments and calculations showed that this structure is easier to power than the rectangular cage which was excited by three sets of orthogonal coils, as previously proposed.

The aim of this work will be to obtain data on the efficiency of the power transfer from the cage to the small detector inside, and to demonstrate the feasibility of the construction of the three mutually orthogonal pick-up detector coils for orientation on

independent powering, at all points inside the cage.

### 3. Single Channel Orientation Independent Powering

In this part of the proposal, we will modify already existing single channel ECG telemetry systems, by adding three mutually orthogonal pick-up coils to the implant. An attempt will be made to optimize the power transfer so that reliable operation will be achieved in the large volume of space inhabited by the animal, for example, the cage of section II. This work will necessitate circuit redesign in order to reduce the power requirements of the implants.

### 4. Three Channel RF Powered Telemetry System

Work on this section will be a continuation of the development of the three channel unit, proposed for the 1974 - 1975 period. Feasibility of the system was demonstrated by a bench model. Most of the work, during 1975 - 1976, will concentrate on the packaging of the unit. The three channels will be used to transmit information about ECG, temperature and pressure. Since incorporation of the pressure channel presents some difficulties in power consumption, we propose to develop a duty cycle switching scheme to minimize this problem, and a bench circuit model is being developed with silicon piezoresistive transducers.

A pressure channel is included in the three channel telemetry unit. An implantable pressure transducer that can last more than a few weeks, with good base line stability, is not commercially available at the present. Our laboratory is developing the implantable pressure transducer for cardiovascular research under our NIH program project, Microelectronics Laboratory for Biomedical Sciences. At the present,

the device has passed engineering and laboratory evaluations. However, the attachment of lead wires and the insulation of the leads from body fluid is being developed. When a satisfactory technique is found to connect the pressure transducer to the telemetry package, the transducer will be used for the proposed three channel telemetry system. If the technological development does not progress as estimated, we will investigate implantable pressure transducers from commercial and research laboratory sources and select the best available unit for use in pressure telemetry.

The tentative specifications of our pressure transducers are:

Size	2mm x 6mm x 1mm
Resistance	2K $\Omega$ bridge
Pressure range	0 to $\pm$ 300mm
Structure	Silicon diaphragm and capsule
Sensitivity	$\approx$ 2.5mV/100mm
Temp. Coefficient	$\approx$ 7mmHg/ $^{\circ}$ C (uncompensated)
Temp. Coefficient	$\approx \pm$ .1mm/ $^{\circ}$ C (compensated)
Hysteresis	1mmHg/30 $^{\circ}$ C

ANNUAL REPORT  
RESEARCH GRANT NDR-36-027-053  
MICROELECTRONIC BIOINSTRUMENTATION SYSTEMS  
July, 1974, to June, 1975

Submitted to  
NATIONAL AERONAUTICS and SPACE ADMINISTRATION

Dr. Wen H. Ko  
Case Institute of Technology  
CASE WESTERN RESERVE UNIVERSITY  
Cleveland, Ohio 44106

**SECTION I**  
**PROGRESS REPORTS**



## A. SINGLE FREQUENCY RF POWERING

### Introduction:

The need for smaller and smaller telemetry transmitters which could be used to transmit physiological information from small animals used in various biomedical experiments today imposes difficult restrictions on the construction of such devices. If the use of the implanted volume is analyzed, it can be found that the battery or equivalent energy storage generally occupies about 50% of the volume, the electronics require 25%, and the rest is usually taken by RF-tank circuit, antennas, connectors and similar accessories. It is therefore, apparent that miniaturization of the electronics itself will not be the complete answer to the problem. In the past few years we have investigated, in our laboratory, the possibility of using the RF field to power the implanted transmitter from the outside, especially when the short range telemetry is used for transmission of data from the animals strapped in chairs or moving in cages. The telemetry system using the external source of energy, which is transmitted into the implant, has one additional advantage in not being limited in operation by battery lifetime and can therefore operate for virtually infinite lengths of time. The description of the system, based on this principle is given in the following sections.

### System Description:

Since it is not desirable to increase volume of the implant

further by adding the receiving tank circuit to the implant, it is necessary to use only one tank circuit for both functions, the RF energy absorption and the data transmission. This is possible to accomplish by the time sharing multiplexing, as shown on the timing diagram given in Figure 1.

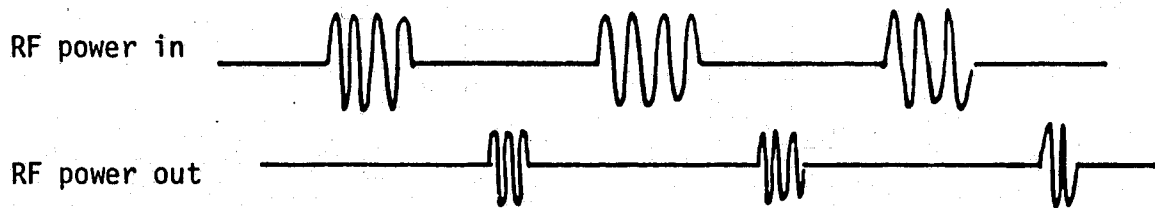


Figure 1. Timing Diagram

The first system built in our lab for the Marine Biomedical Institute in Galveston under NASA contract number NGR-36-027-053 worked well and had the following block diagram, as shown in Figure 2.

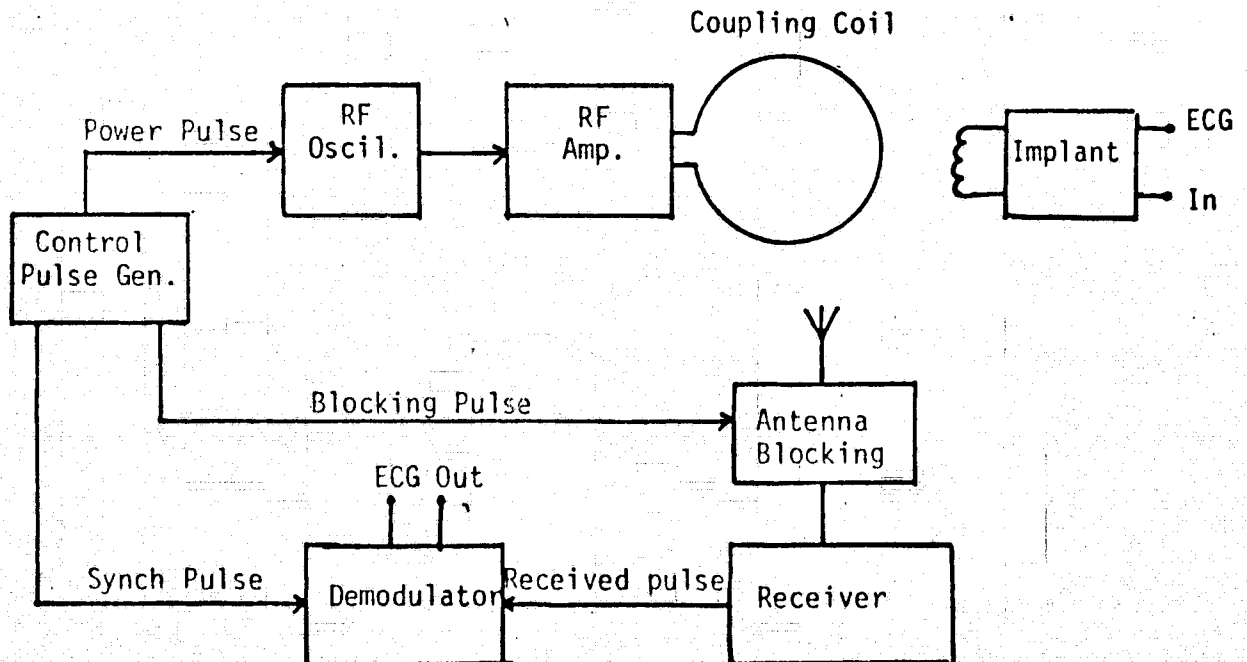


Figure 2. Telemetry System Block Diagram

The system was used to transmit the ECG signal from a Rhesus monkey strapped in a chair. The RF coupling coil was slipped on the chair so that the axis of the coil was parallel to the spine of the monkey. The operation of the system is apparent from the timing diagram given in Figure 3.

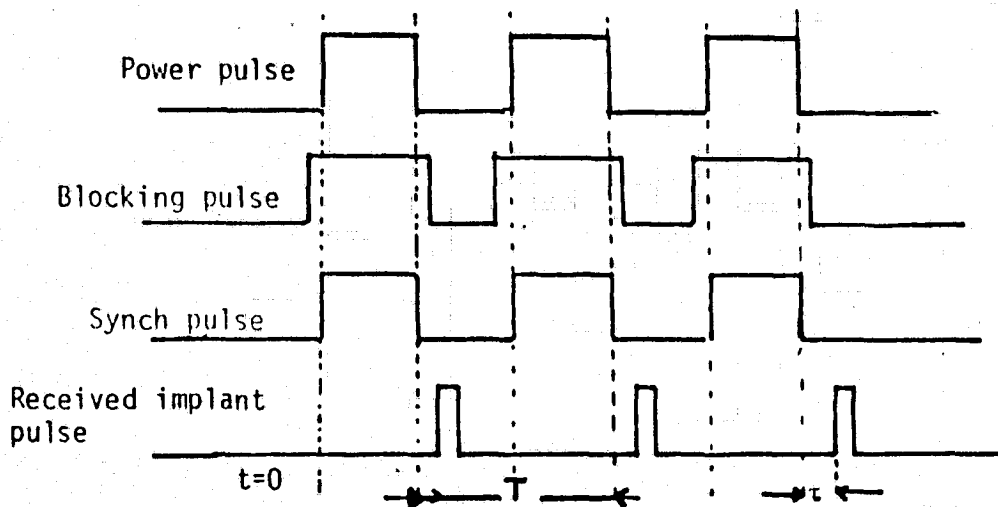


Figure 3. System Timing Diagram

The information about the ECG signal which is applied to the input of the implant is sampled once every period which has the length,  $T$ , and is converted into the delay  $\tau$  of the transmitted pulse. Therefore, the position  $\tau$  of the transmitted pulse is modulated (pulse position modulation) in correspondence to the input voltage. Since the synchronizing pulse for the implant is derived from the trailing edge of the RF power pulse, the accuracy of the transmitted information from the implant is not affected by any variations in the pulse widths. The described-signal format can be easily extended into

the multichannel operation simply by further time multiplexing. The three channel system is presently being investigated where the following pulse format is employed, Figure 4.

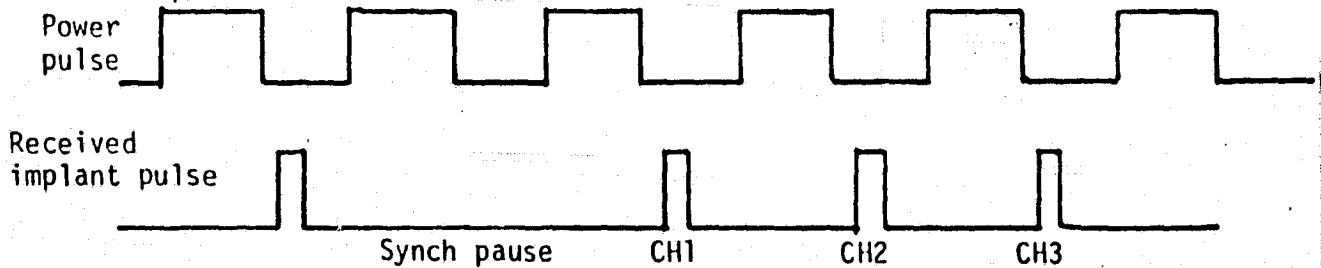


Figure 4. Three Channel RF Powered System Signal Format

Since all of the circuitry filling up the blocks in the diagram in Figure 2 is conventional, with the exception of the circuits for the implant, our description will be dealing in more detail only with the electronics of the implant.

#### Description of the Implant:

The most important section of the implantable transmitter is the oscillator. The complication here is the requirement that the same tank circuit has to be used for detection of the RF power and also for the transmission of the signal. In addition, the circuit has to generate a trigger pulse coinciding with the trailing edge of the RF pulse which is needed for synchronization. The complete circuit diagram for the oscillator is given in Figure 5.

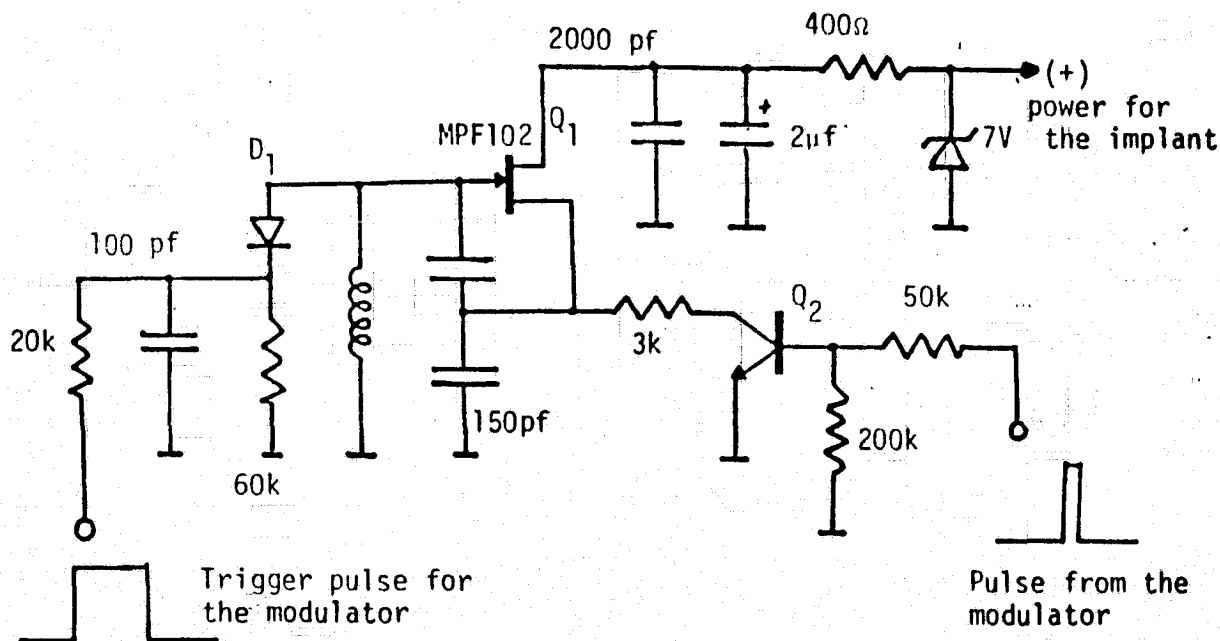


Figure 5. Oscillator Circuit Diagram

The FET MPF 102 is used as the RF detector, since the gate and drain serve as a diode when the transistor  $Q_2$  is turned off. The charge is stored in the capacitor and the voltage is stabilized by the Zener diode. A separate RF detector is used to generate the trigger pulse for the modulator. When the transistor  $Q_2$  is turned on, the FET works as in a conventional Colpitts oscillator. At this moment the RF voltage generated across the inductor  $L$  is not high enough to retrigger the modulator. The modulator circuit diagram is given in Figure 6.

Here the voltage to pulse position conversion is accomplished by means of a Miller integrator (Transistor  $Q_3$ ). The voltage ramp generated at the collector of the  $Q_3$  (after the trailing edge of the trigger pulse) is terminated as soon as the transistor  $Q_4$  is saturated. The time of integration is, therefore, proportional to the voltage

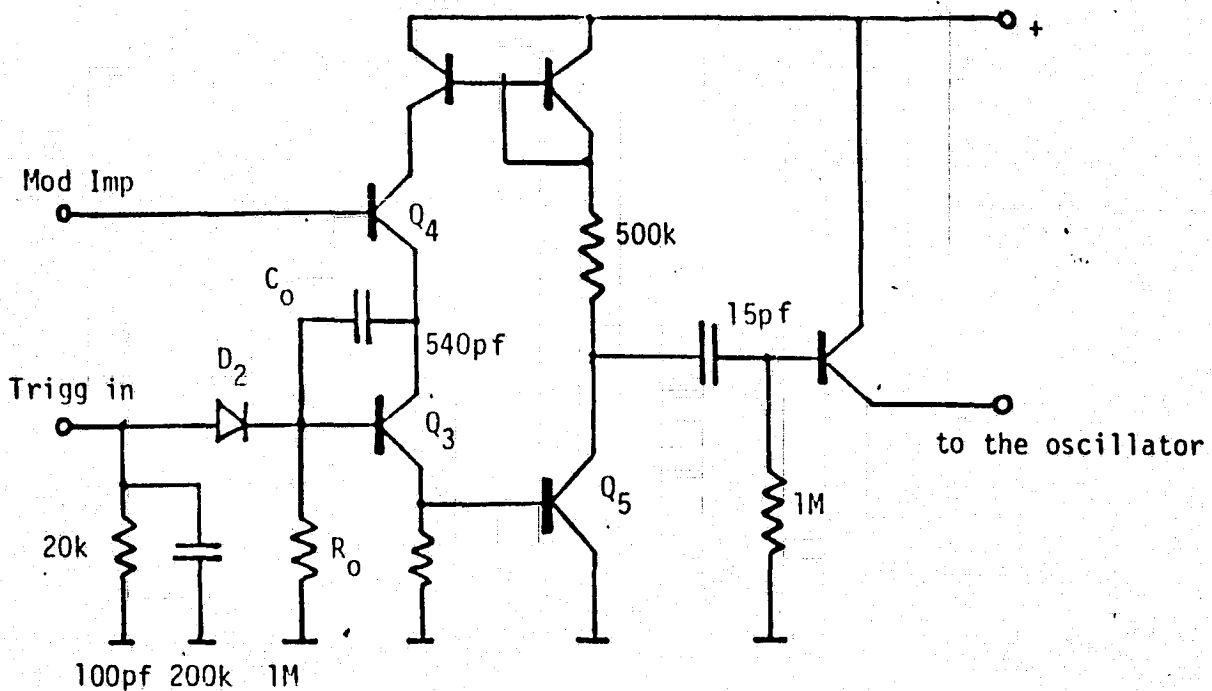


Figure 6. Modulator Circuit Diagram

at the base of  $Q_4$ , which is the input of the modulator. When the  $Q_4$  is saturated, the  $Q_3$  and  $Q_5$  are turned off and the pulse spike appears at the output of the modulator. This pulse then triggers the oscillator and an RF burst is transmitted out from the implant. The signal which is used for the modulation can be obtained from a variety of sensors. In our case we used a standard ECG instrumentation amplifier to amplify the ECG signal up to the necessary amplitude which is required for the modulator. It should be stressed, at this point, that attention has to be given to the design of the input circuit of the high gain amplifier to avoid RF saturation during the powering. Usually a simple RC filtering network is sufficient. More complicated schemes using sampling and blocking techniques are under



investigation. The implant was packaged in three flat packs with RF tank coil wound on a ferrite core as shown in the photograph in Figure 7.



Figure 7. Photograph of the Implant Unit

## B. RF POWERED CAGE DESIGN AND CONSIDERATIONS

### Introduction:

The purpose of this report is to describe the work which was performed in order to gain enough information to build an RF powered cage. The first section describes the RF detector which was used to measure the RF field, and the second section describes measurements and results performed on two different cage designs. However, at this point, satisfactory results were only obtained for the cage with open sides. The measurements on the completely enclosed cage indicated that numerous parasitic modes of oscillation were generated, resulting in a strongly nonuniform field throughout the cage.

### Calibration of Detecting Probe:

As shown in the last report, the detecting probe is a half-wave rectifying circuit with a pick-up coil which has the same capture aperture as that in the implant (0.75 sq. in.). This probe is being calibrated by putting it in the center of a single turn circular loop while the field is varied by varying the loop current. The obtained calibrating curve is shown in Figure 8. By using this curve, it will be easy to tell the field value at any location from the pick-up voltage readings.

### Generation of Circular Polarized Magnetic Field by a Symmetrical Two-

#### Coil Configuration:

In the last report, measurements on a one meter cubical cage with two coils which are driven at 30 MHz had been done. As shown in

Figure 9 and Figure 10, the two coils consisted of four 0.5 inch diameter rods with part of the cage as their path, and each was tuned in series by two 50 pf variable capacitors. This structure, tapped 2 inches from one side of the enclosure, formed two coils driven in phase and was expected to produce a uniaxial magnetic field. But due to the path between two coils, parasitic asymmetrical modes were generated resulting in an unsymmetrical magnetic field.

Some of the measurements on the magnetic field inside the cage are repeated to re-examine the possibility of obtaining symmetrical magnetic field. Figure 11 shows the relative output along the Z-axis in the Z-direction. In the figure, the dashed line represents the new result. With proper tuning of the capacitors the new result shows a more or less symmetrical field. Figures 12 and 13 show the Z-directed field in the X and Y direction, respectively. From the results of the repeated measurements we find that for this configuration it is difficult to tune the capacitors properly to obtain symmetrical modes of operation. Another configuration with two diagonally located symmetrical coils which can generate a circular polarized magnetic field is then proposed. As shown in Figure 14, two sets of rods, acting as the coils, are located diagonally showing the feeding lines for one set of coils. The required metal enclosure forms the outer sides. If the signal is fed into the two sets of coils and differs in phase by  $90^\circ$ , then it will result in a circular polarized magnetic field which can give more opportunity for the detector in the implant to get constant pick-up voltage.

Experiments on the said configuration have been done. The present structure is a 50 cm cubical box with only the top and bottom sides.

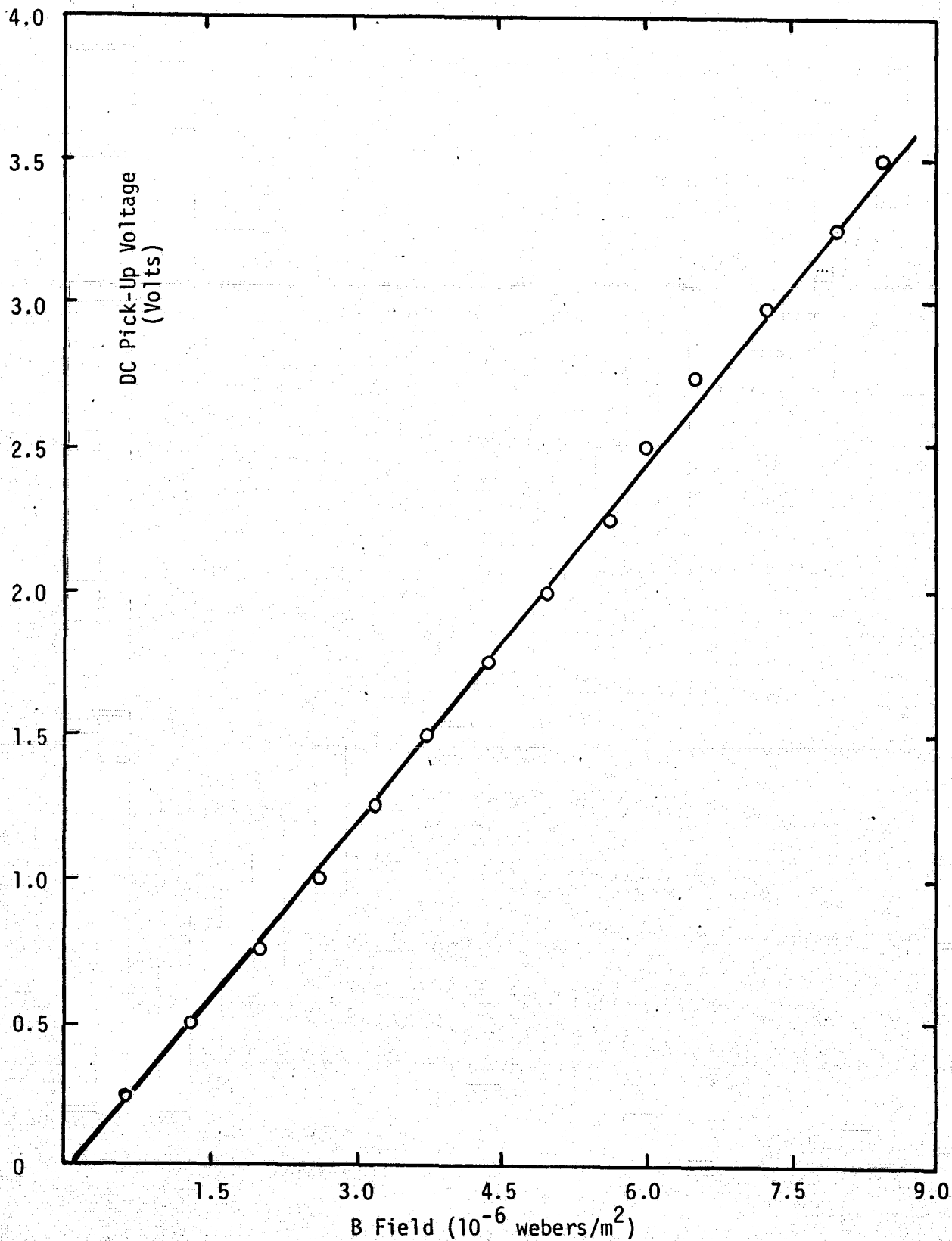
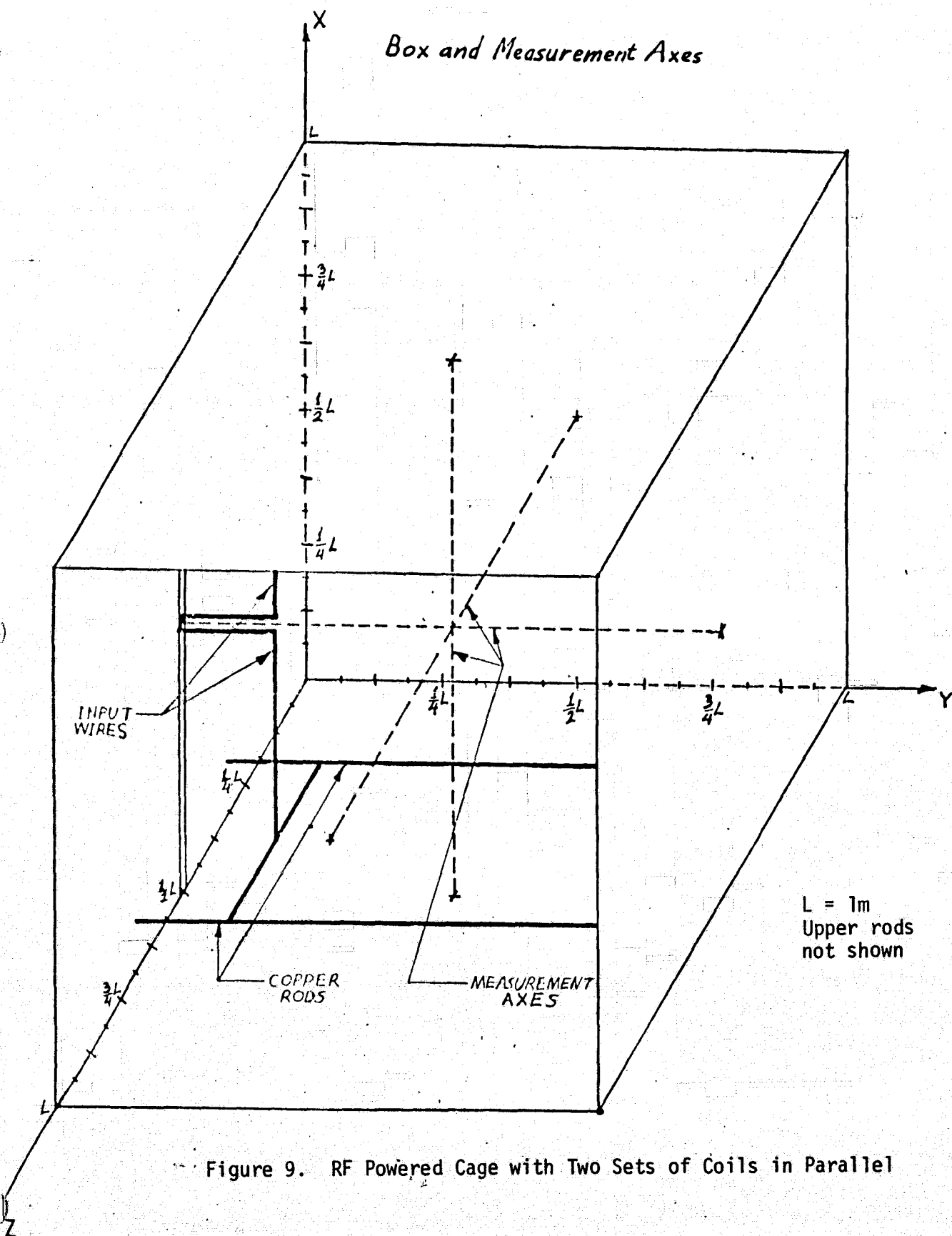
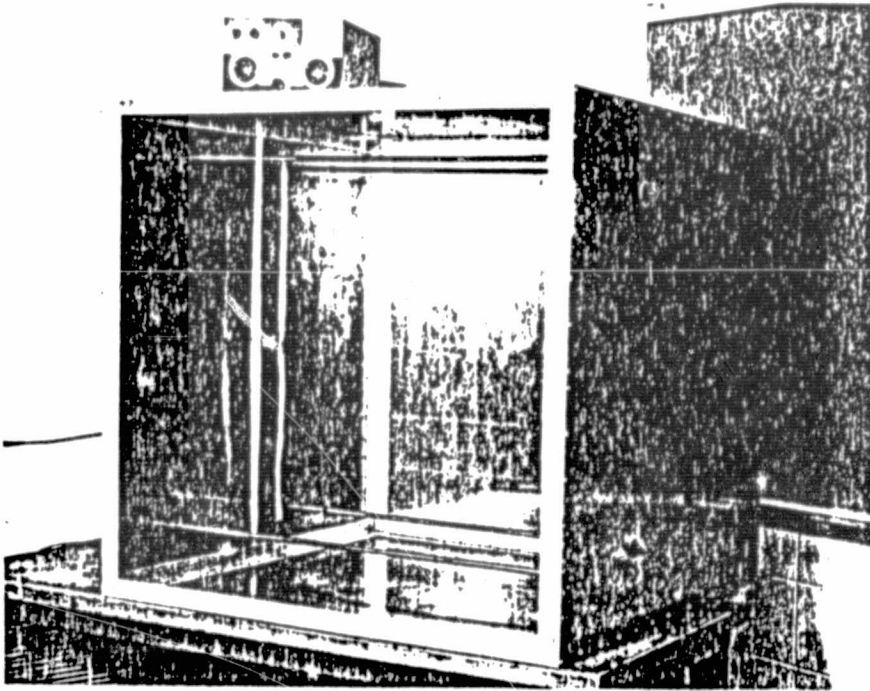


Figure 8, Calibration Curve for the Detecting Probe





ORIGINAL PAGE IS  
OF POOR QUALITY

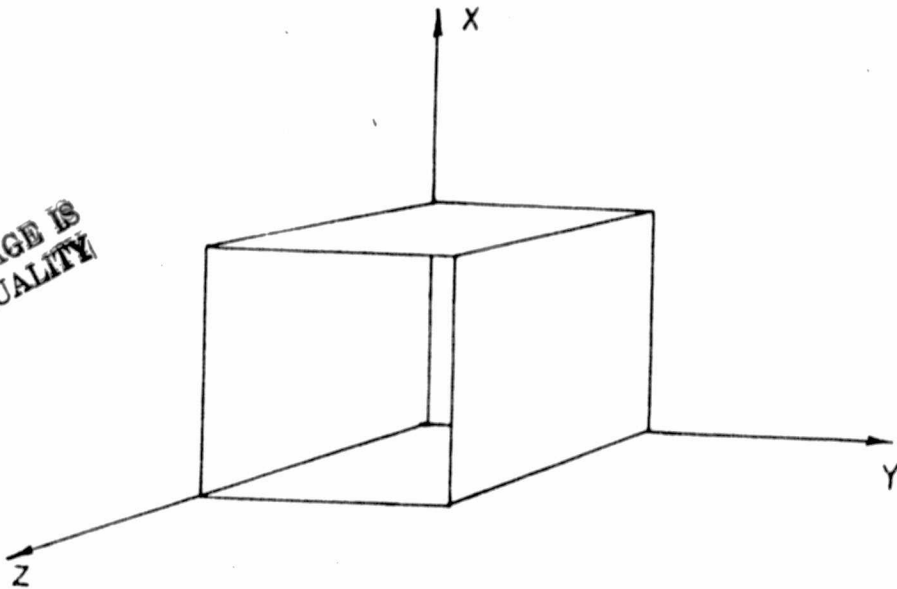


Figure 10. RF Powered Cage with Two Sets of Coils in Parallel



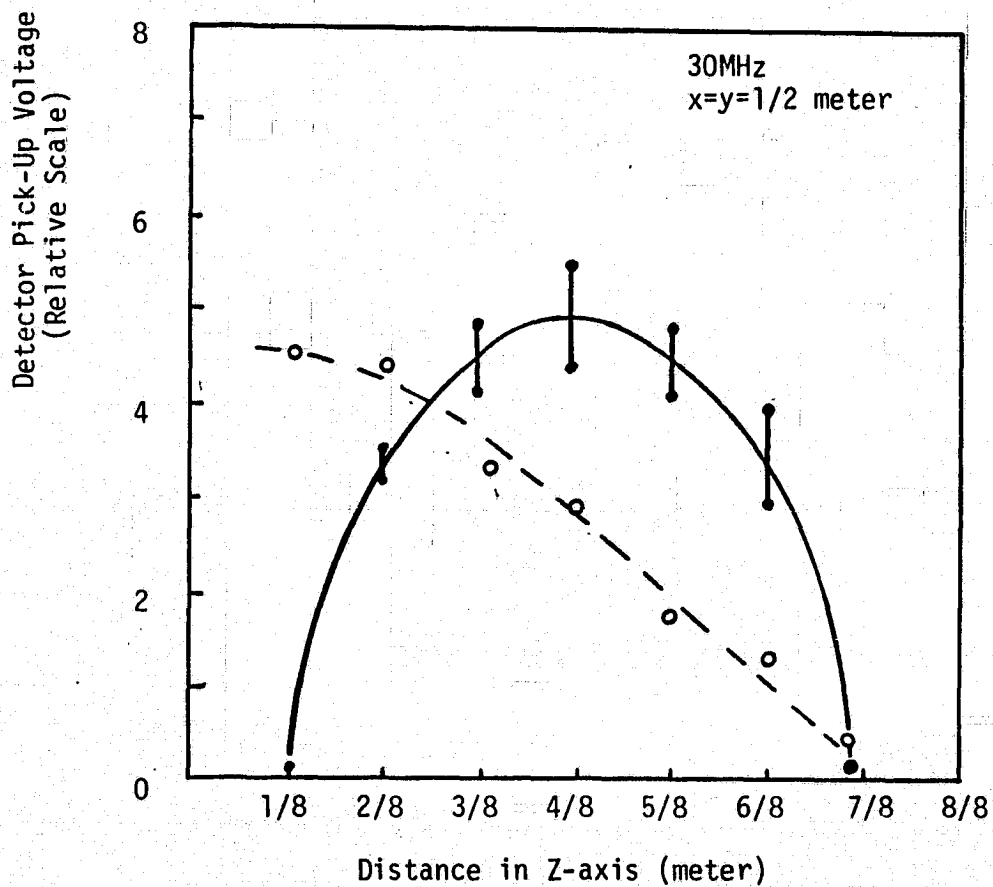


Figure 11. Z-directed Field in Z-axis

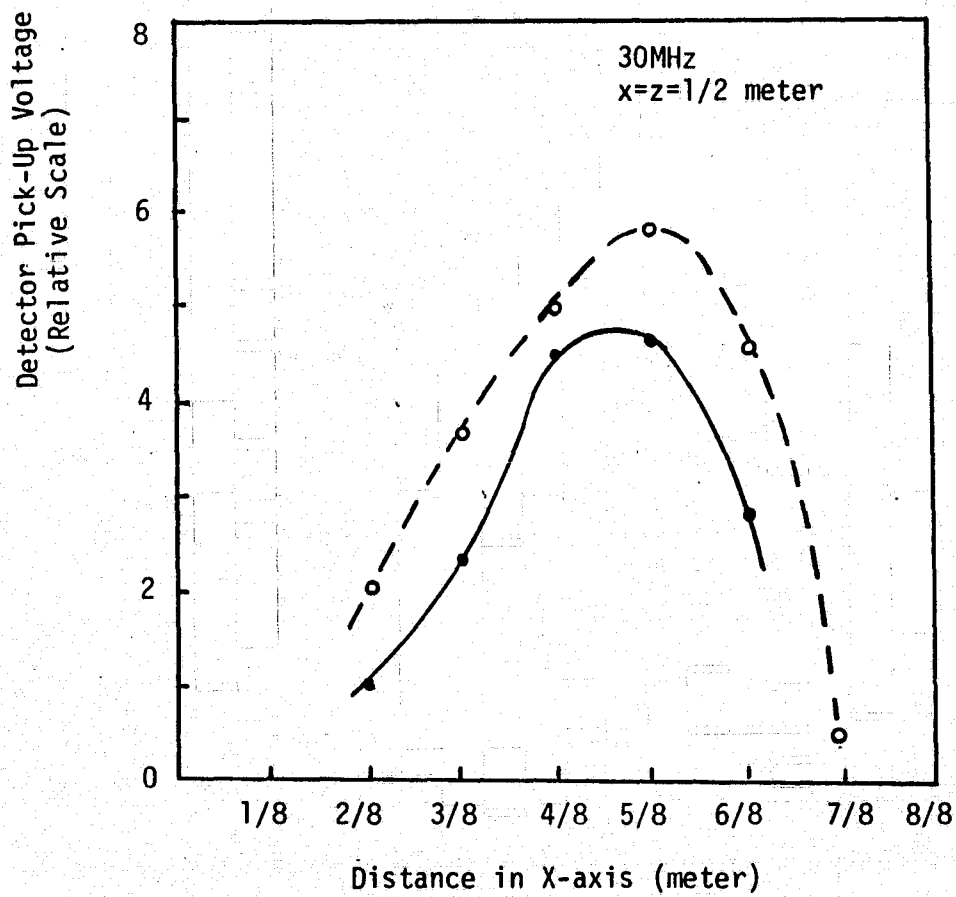


Figure 12. Z-directed Field in X-axis

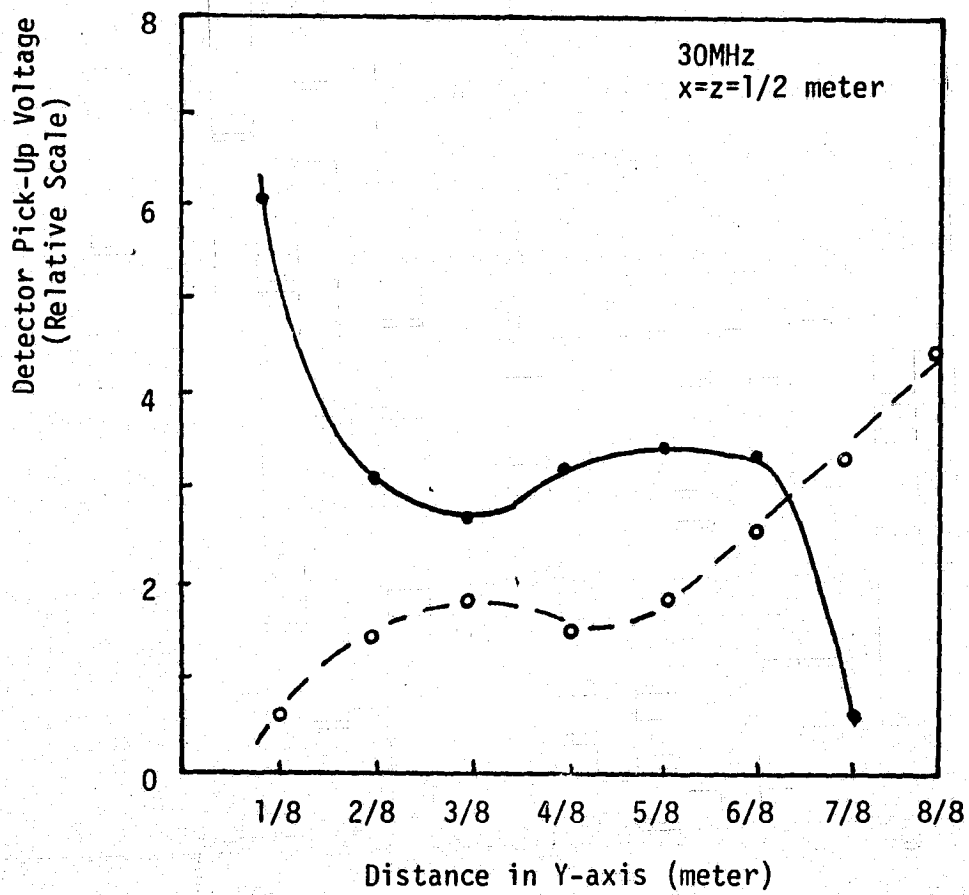


Figure 13. Z-directed Field in Y-axis

Balanced voltage is fed into one set of the coils while the other set of coils remains open circuited. As shown in Figure 15a, capacitors C1 and C2 are for tuning, while the tappings of the feeding lines are used for impedance matching. Five watts of RF power, at the frequency range of 20-30 MHz, are delivered to the box. The coordinates for measurement are defined in Figure 15b. Tuning capacitors C1 and C2 must be equal in order to have the current only pass through the driven rods. Otherwise, unsymmetrical modes of operation, with current from one of the driven rods passing through the other rods, will result in an asymmetrical field distribution. Figure 16 shows the Y-directed relative pick-up voltage when the box is tuned in such a way that C1 is larger than C2. From the curve, one can see the largely asymmetrical field distribution. If, in the tuning procedure, C1 and C2 are carefully adjusted, then a symmetrical distribution generated by the driven rods can be obtained as shown in Figure 17. The work now being done is aimed at generating a circular polarized field by feeding the signal, which is delayed by one-quarter of the wavelength, to the other pair of rods.

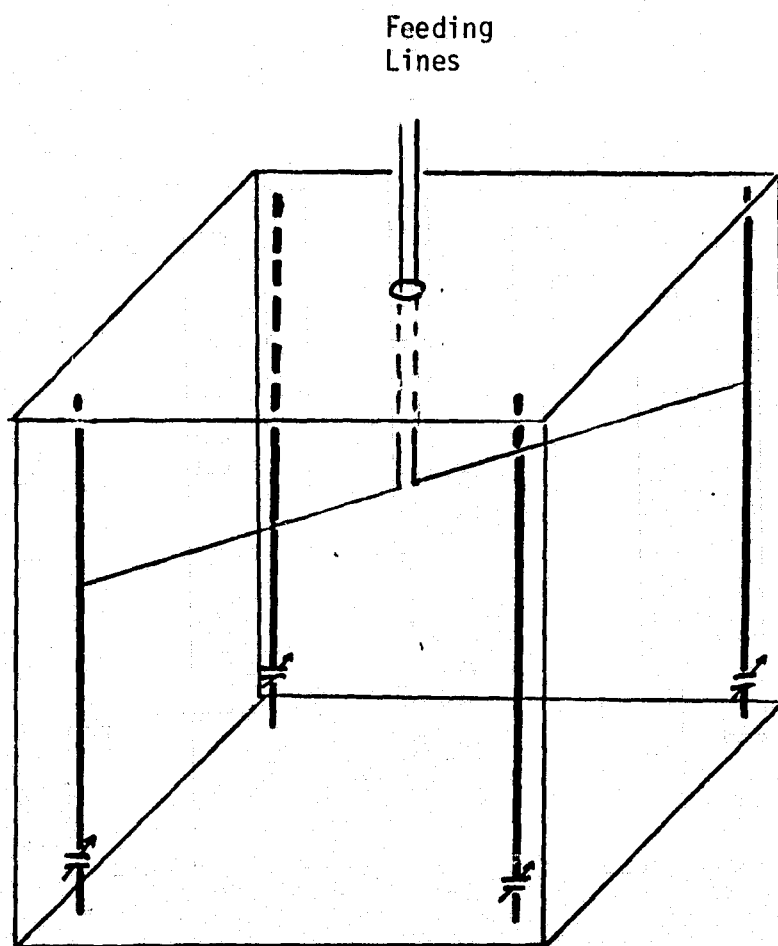


Figure 14. RF Powered Cage with Two Sets of Diagonally Located Coils

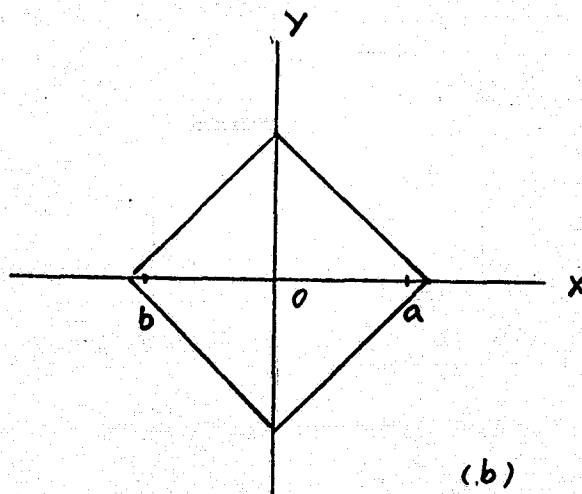
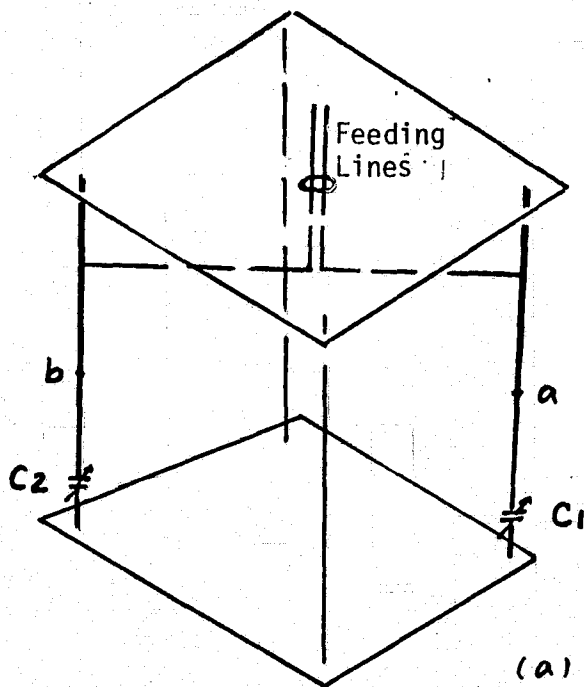


Figure 15. Coordinates for the Cage



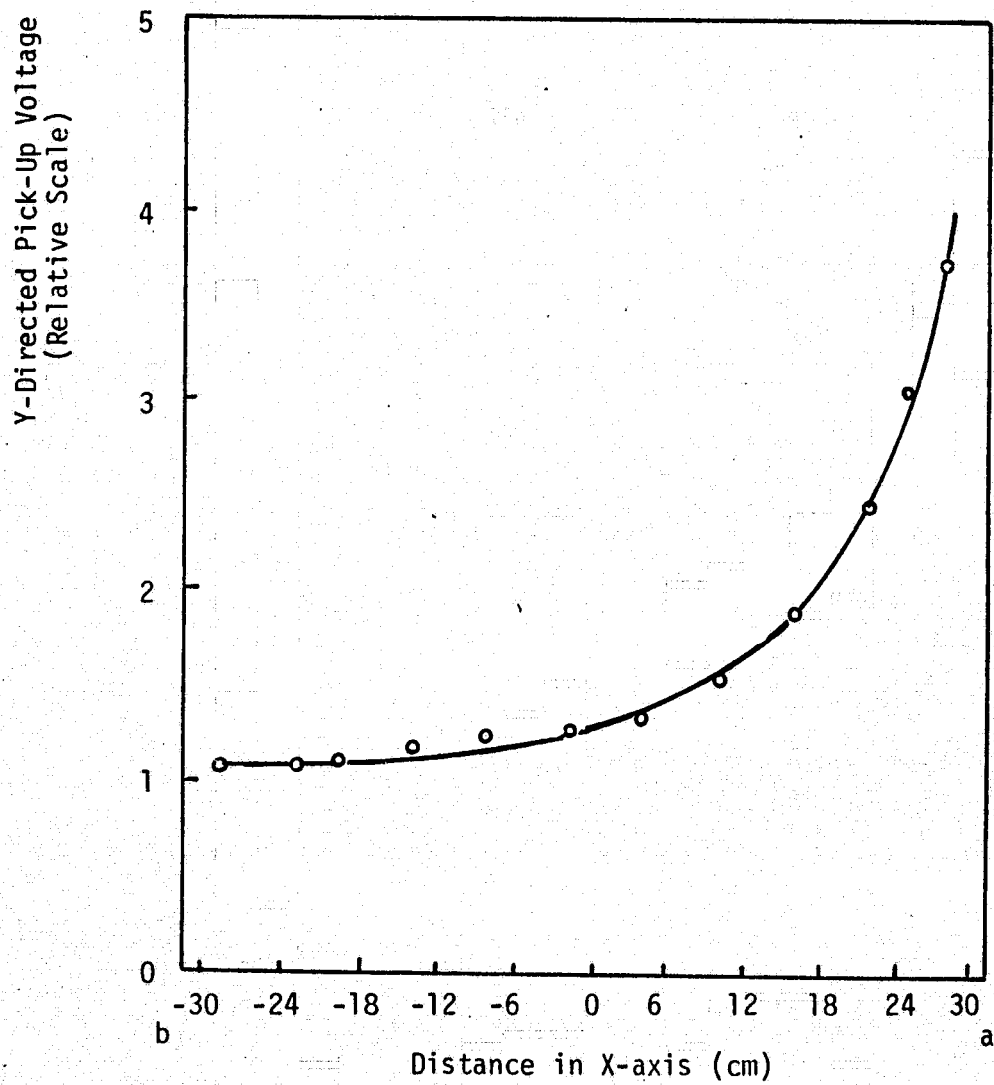


Figure 16. Y-directed Field in X-axis with  $C_1 > C_2$

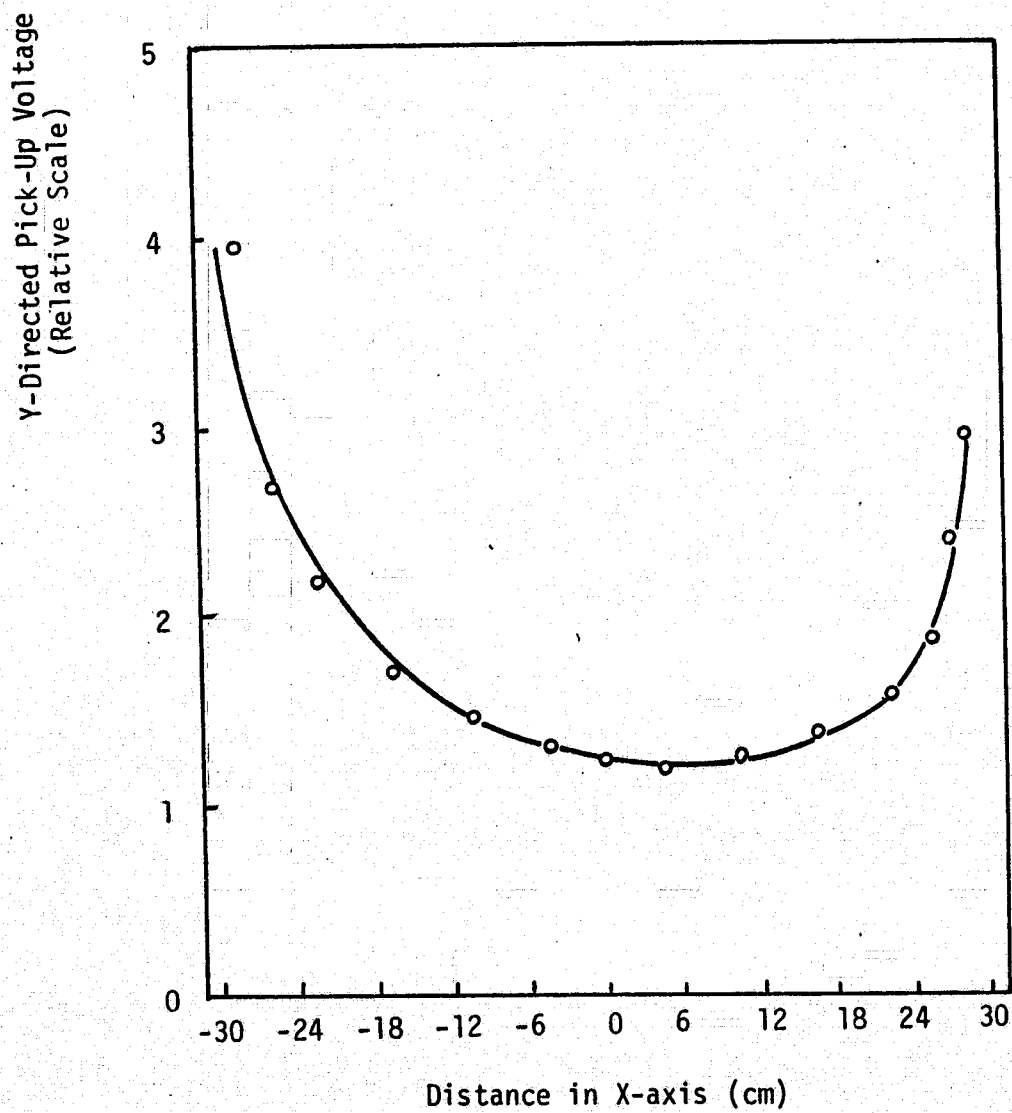


Figure 17: Y-directed Field in X-axis with  $c_1 \approx c_2$

### C. INGESTIBLE TELEMETERING SYSTEM

This part of the report summarizes the progress made on the development of an ingestible temperature telemetry system shown in Figure 18. The report includes the pulse frequency modulator of the transmitter and the digital processing unit of the receiving unit. The system's performance was evaluated in ingestion and implant experiments.

#### Pulse Frequency Modulation:

The M-7 pulse frequency modulator, Figure 19, was designed to modulate a K-6 oscillator, Figure 20, and typical performance characteristics are given in Table 1. A packaged unit standing at room temperature has a lifetime of more than three months. Evaluation of the transmitter was performed in ingestion and implant experiments as described below. The packaged M-5 and M-7 units are shown in Figure 21. The transmitter can be encapsulated and/or epoxied for protection in capsules made of ABS, Black Delrin<sup>TM</sup> or glass, Figure 22. Performance of the transmitter in different packaging methods and materials are still undergoing tests.

#### Digital Processing Unit, Figure 23:

The digital processing unit was built and tested. The completed unit chassis and packaging are given in Figures 24 and 25. The unit consists of five boards:

1. Control logic board, Figure 26
2. Pulse period discriminator board, Figure 27
3. Digital counter and logic board, Figure 28
4. D/A converter board, Figure 29
5. Power supply board

A brief description of these boards is given below.

#### Control Logic Board:

This board performed the following functions:

1. Pulse amplitude discrimination, Figure 30. This discriminator is the first series discrimination scheme in the processing unit. The capacitor,  $C_1$ , charges up to the incoming pulse amplitude through the buffer OA1. OA3 is intended to compensate for the voltage drop of  $R_1$  and base to emitter junction diode of  $Q_1$ . The intended threshold for discriminating an incoming signal is adjusted by  $R_8$  and COMP1 acts as the comparator.
2. Pulse width discrimination, Figure 26. This discriminator consists of monostable multivibrators, MM1 and MM2, whose pulse width is preset at  $t_1$  and  $t_2$ , respectively. This will set up a time window for acceptance of a pulse with pulse width  $\tau$ , satisfying  $t_1 < \tau < t_1 + t_2$ .
3. Error counter, Figure 26. The error counter counts the number of pulses coming in once an error signal beyond the acceptable pulse period range is detected. During the counting period there will be no pulse output and the digital display will keep the last acceptable value on display. The error counter will be

filled by seven counts (1-1-1) and the pulse period discriminator will be cleared to restart its function. Thus, the error counter is able to discriminate a sudden burst of error signals (less than seven counts).

4. Logic circuit, Figure 26. This acts as the interfacing unit between the different discrimination schemes to perform the desired functions.

#### Pulse Period Discriminator Board:

This discriminator will store the last incoming pulse period and compare it with the present signal. A presettable range of period width will allow the discrimination between expected pulse period variation and noise signal. This unit combines with the control logic and will perform the desired pulse discrimination.

#### Digital Counter and Logic, Figure 28:

This unit consists of timing circuitry which will gate the display from 0.5 - 15 sec. intervals. The counter is a presettable unit so that a reference number can be dialed in (such as the 37°C normal body temperature). This enables the display to show the variation from the preset reference. Thus, the sensitivity of the counter can be increased with the same number of digits and variation in body temperature can be easily recognized.

#### D/A Converter, Figure 29:

This module is designed to convert the digital output as on the

digital display to analog signal. This provides for analog display of the temperature information as well as storage on the chart recorder.

#### Ingestion Experiments:

Two ingestion experiments were performed, using a male dog weighing twenty-five pounds. Each M-7 transmitter was powered by a 212 mercury cell. The units were packaged and encapsulated in the Black Delrin<sup>TM</sup> capsules. The capsules were then coated with silastic for protection.

In each experiment the subject was made to ingest the transmitter. The transmitter signal was received by an AM receiver and the temperature information was demodulated by the M-7 unit and recorded on a strip chart. A portion of the recording, when the capsule was in the anterior GI tract and the subject was drinking, is given in Figure 31. The capsules were excreted after thirty to forty hours in the GI tract and were then recovered.

Sporadic noises and loss of signal interfering with the demodulation performance were caused mostly by sudden movement of the dog. Signal receiving and demodulation were successful for 95% of the time, Figure 30.

#### Implant Experiment:

In the implant experiment and epoxy encapsulated transmitter was implanted in the pericardial cavity of a female New England white rabbit. Continuous temperature information, over the first

two week period was recorded.

Gradual unidirectional shifting of the transmitter RF and the temperature information baseline were recorded after the initial two weeks. The transmitter ceased to operate four weeks after the implantation. The recovered transmitter was analyzed for cause of failure.

Appreciable water leakage into the battery through a large bubble in the epoxy bed was found. This, mixed with the leakage electrolyte from the battery, provided a 'shorting' current path. Thus, the battery was exhausted prematurely.

Different packaging methods and materials are being tested to improve the lifetime of the transmitter for implantation. A second implant experiment using Kraton as the coating material is being carried out.

PARAMETER	VALUES	REMARKS
Size and weight	0.22 X 0.28" 1 3/4gm	with 212 Mercury cell
Power supply and drainage	1.35V 4 - 6 $\mu$ A 5.4 - 8.1 $\mu$ W	212 Mercury cell } 37° - 50°C
Radio frequency f	130 MHz	
Pulse width t	10 $\pm$ 1 $\mu$ sec	25° - 50°C
Pulse period $\tau$	3625 $\mu$ sec	Measured at 37°C
Sensitivity	95 $\mu$ sec/°C	Measured at 37°C
Straight line linearization @ 37°C	<0.05°C	Error in the $\pm$ 5°C extremity
Stability $\Delta f$ $\Delta \tau$	$\pm$ 0.5 MHz $\pm$ 10 $\mu$ sec	in a day Equivalent to $\pm$ 0.05°C at 37°C

Table 1. M-7 Performance Characteristics



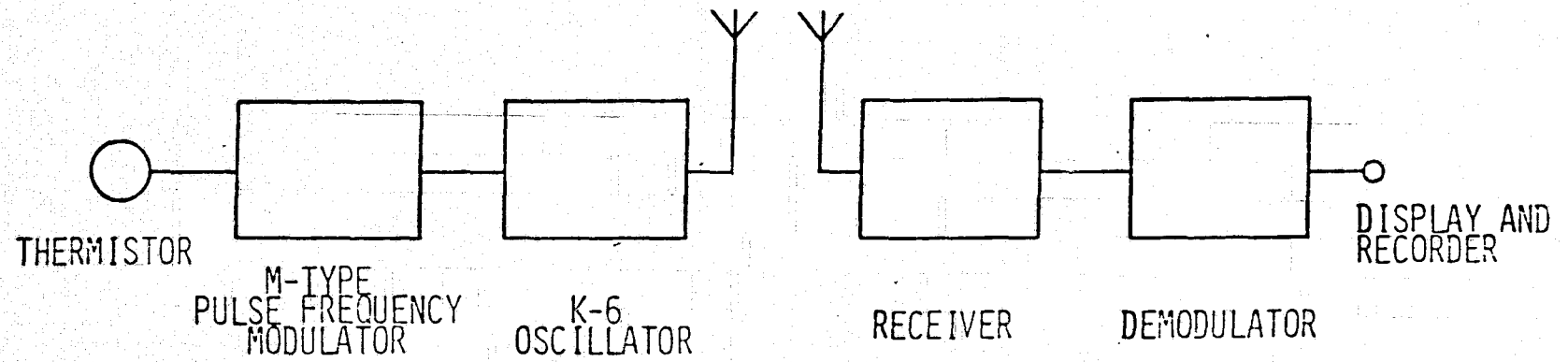


Figure 18. Telmetry System Block Diagram

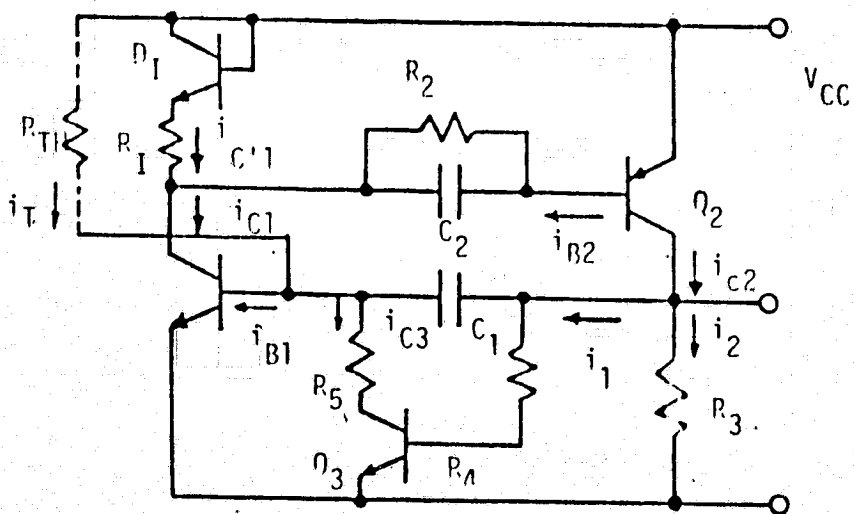


Figure 19. M-7 Pulse Frequency Modulator

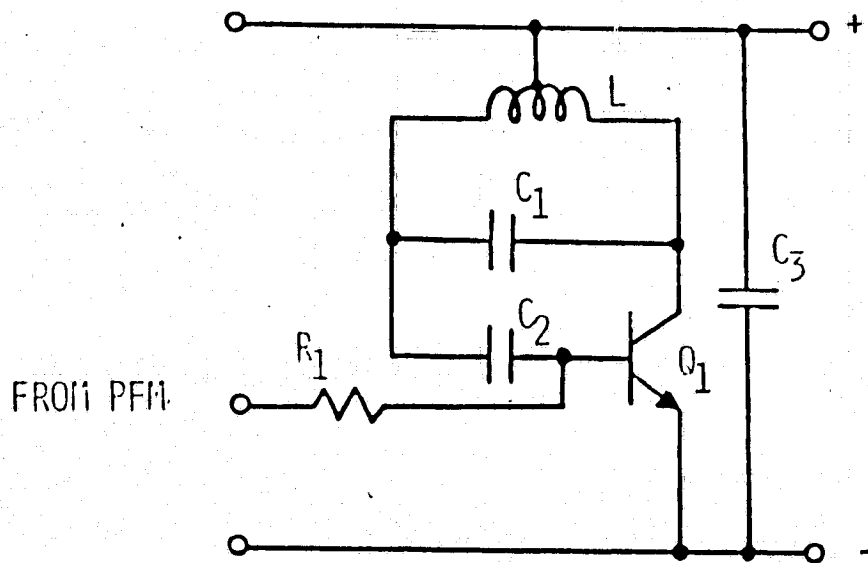
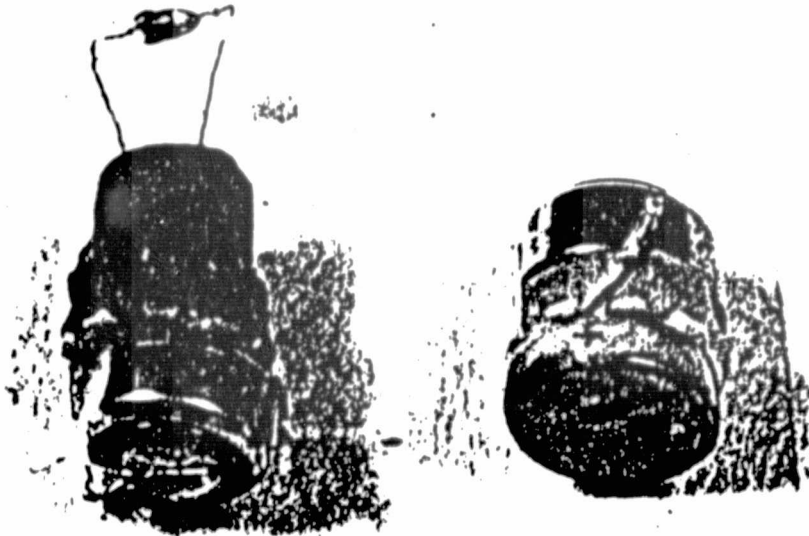


Figure 20. K-6 P Pulse Modulated RF Oscillator



ORIGINAL PAGE IS  
OF POOR QUALITY

Figure 21. Packaged M-7 and M-5 Transmitter

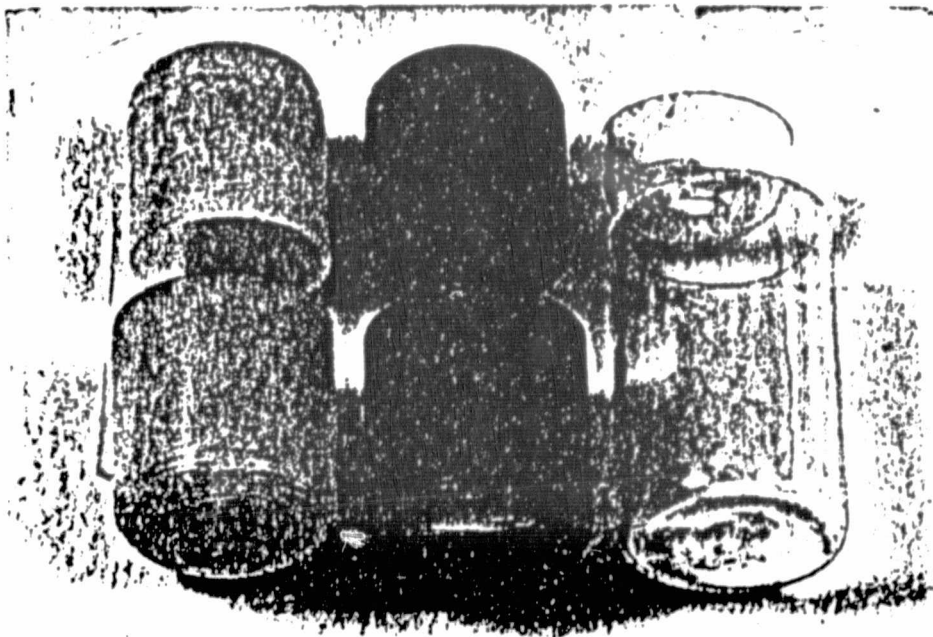


Figure 22. Capsules for M-7 Transmitter  
(ABS, Black Delrin<sup>TM</sup>, Glass)

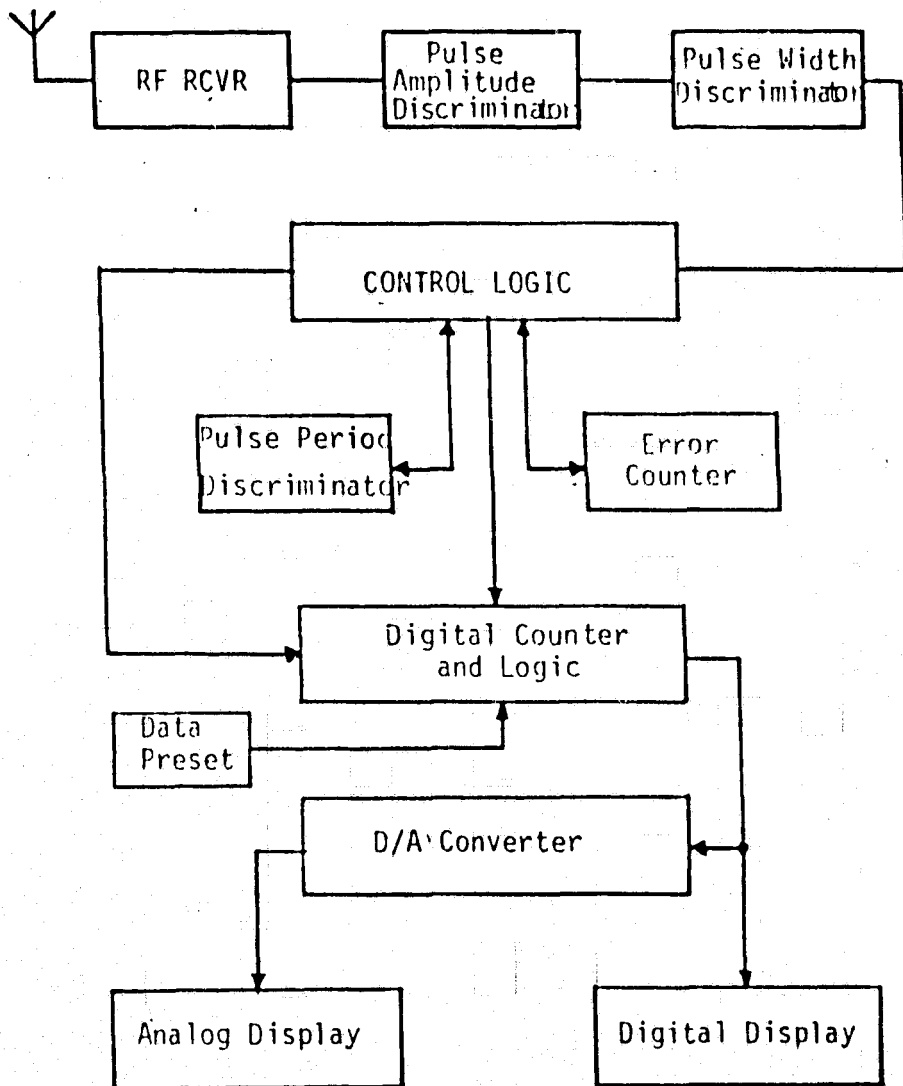
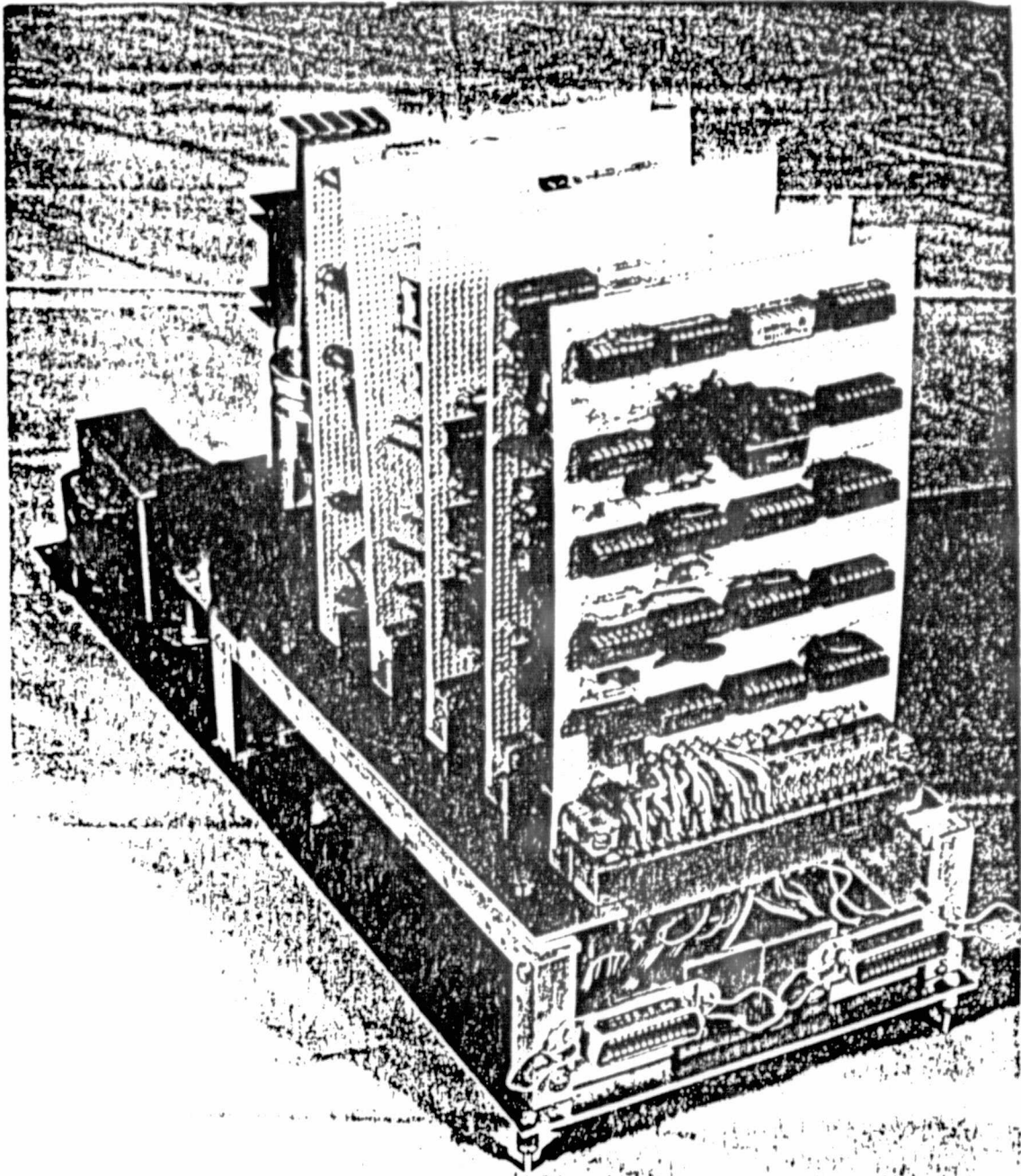


Figure 23. Digital Processing Unit Block Diagram



ORIGINAL PAGE IS  
OF POOR QUALITY

Figure 24. Chassis Mounting of Circuit Boards of  
M-7 Digital Processing Unit

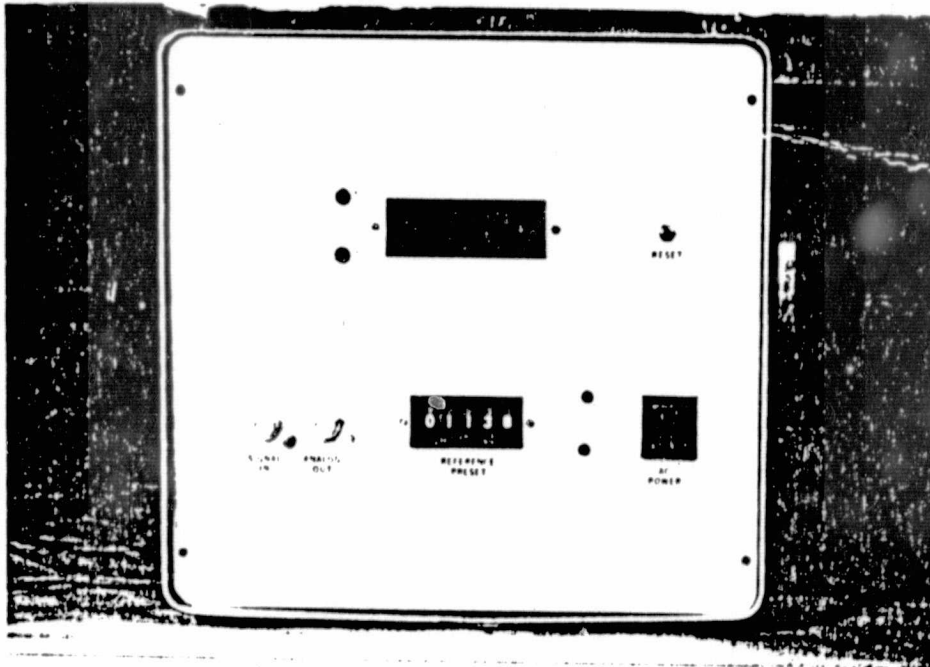


Figure 25. Instrument Box Front Panel Layout of  
Digital Processing Unit



ORIGINAL PAGE IS  
OF POOR QUALITY

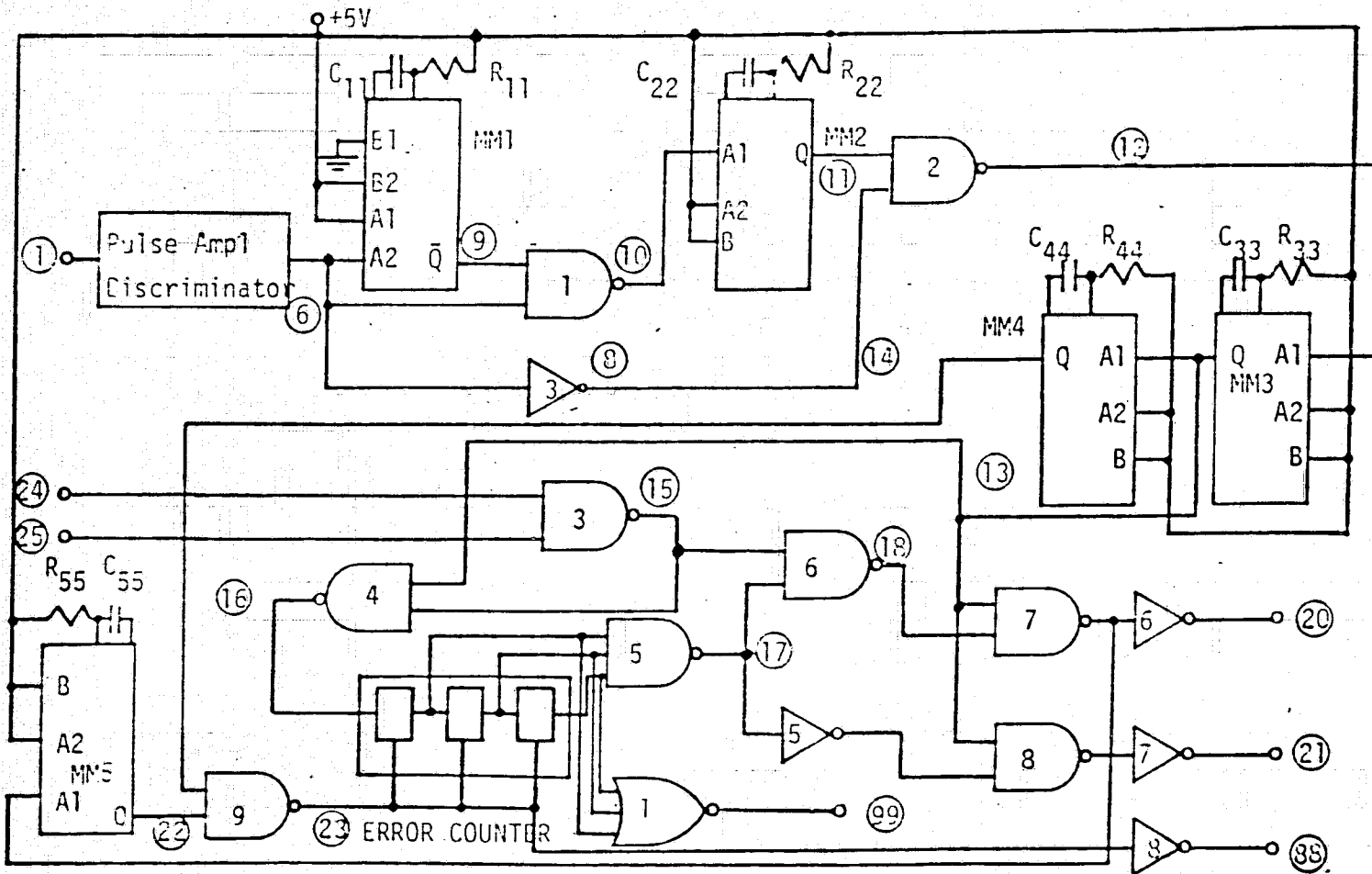


Figure 26. Control Logic Circuit Diagram



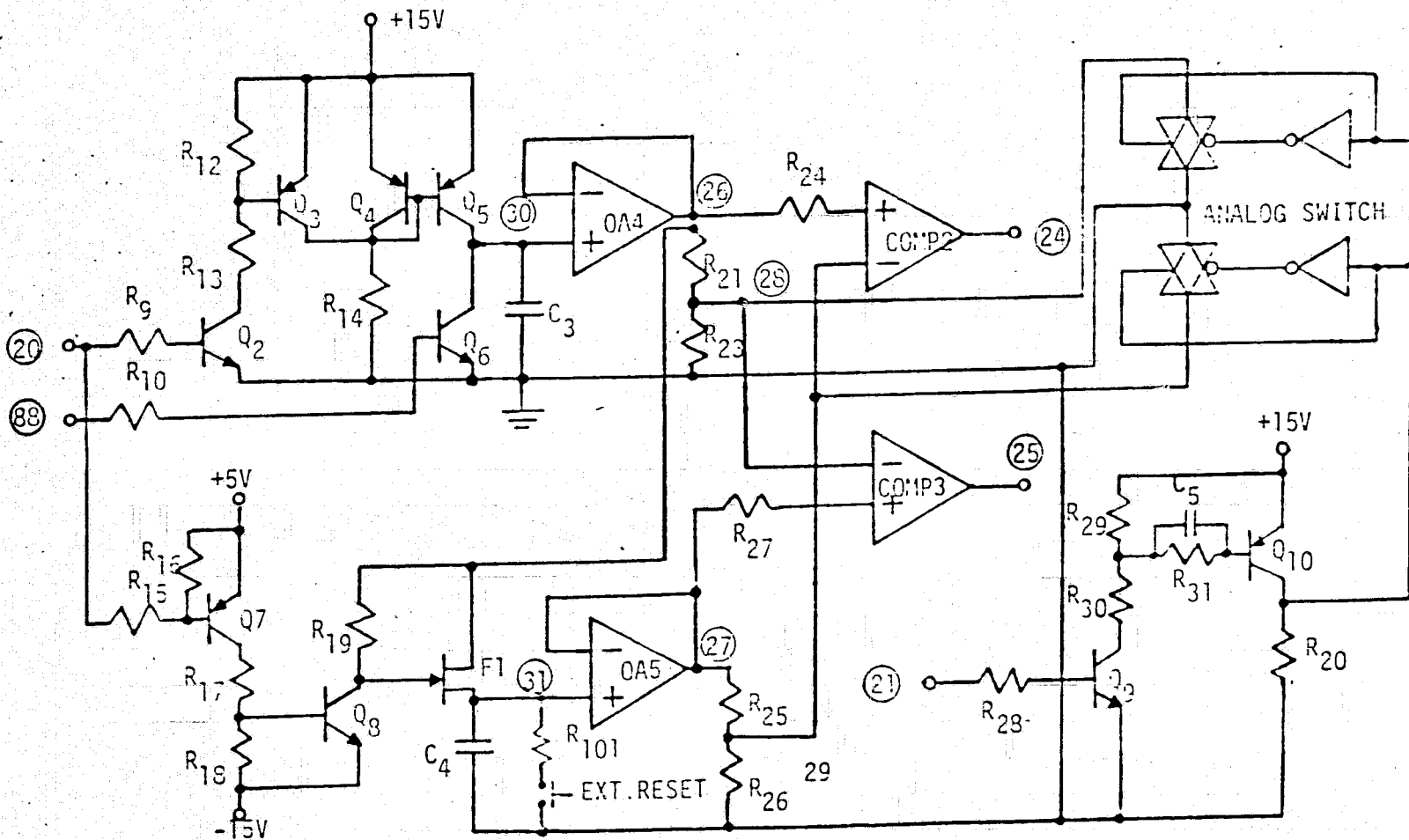


Figure 27 . Pulse Period Discriminator Circuit Diagram

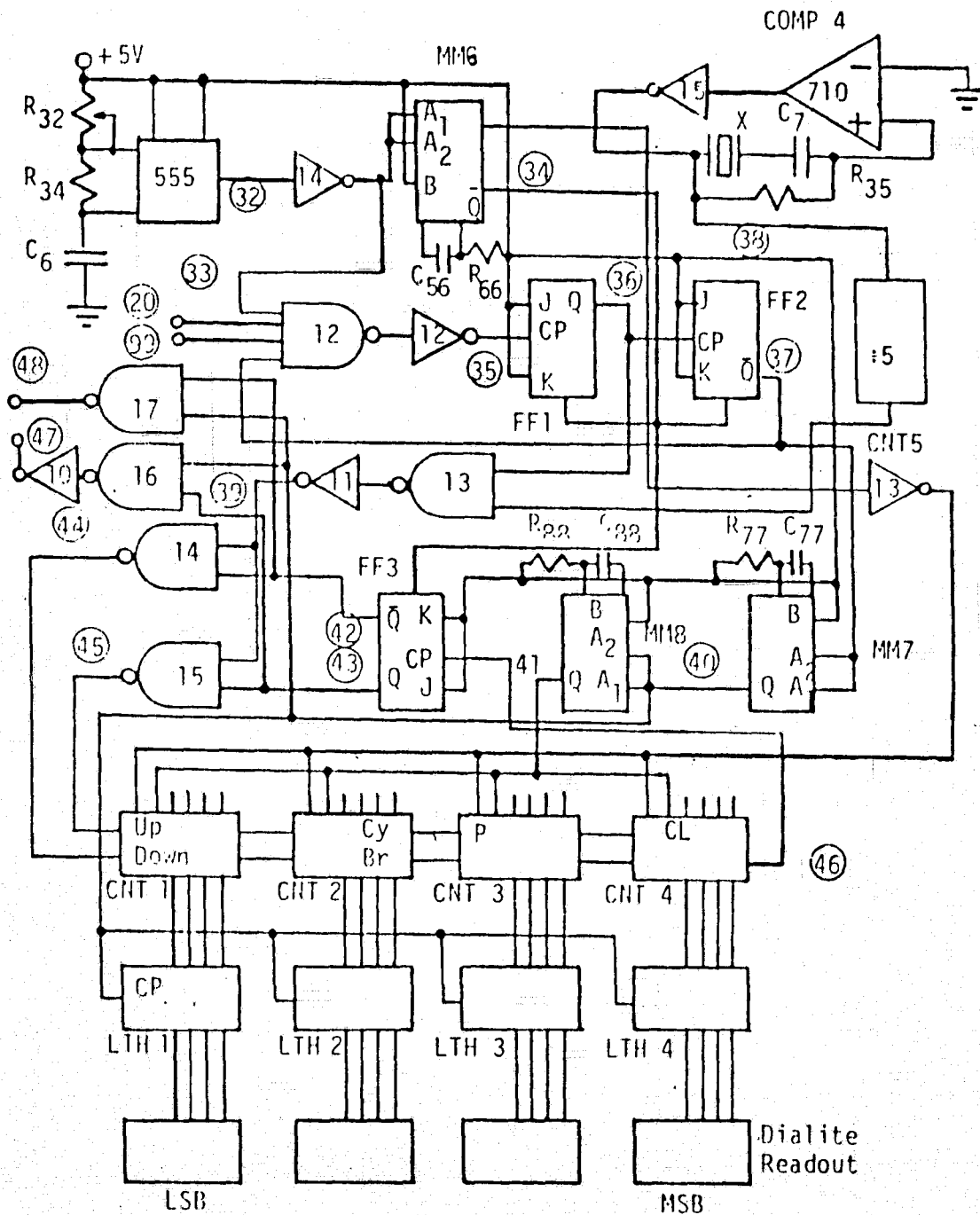


Figure 28. Digital Counter and Logic Circuit Diagram

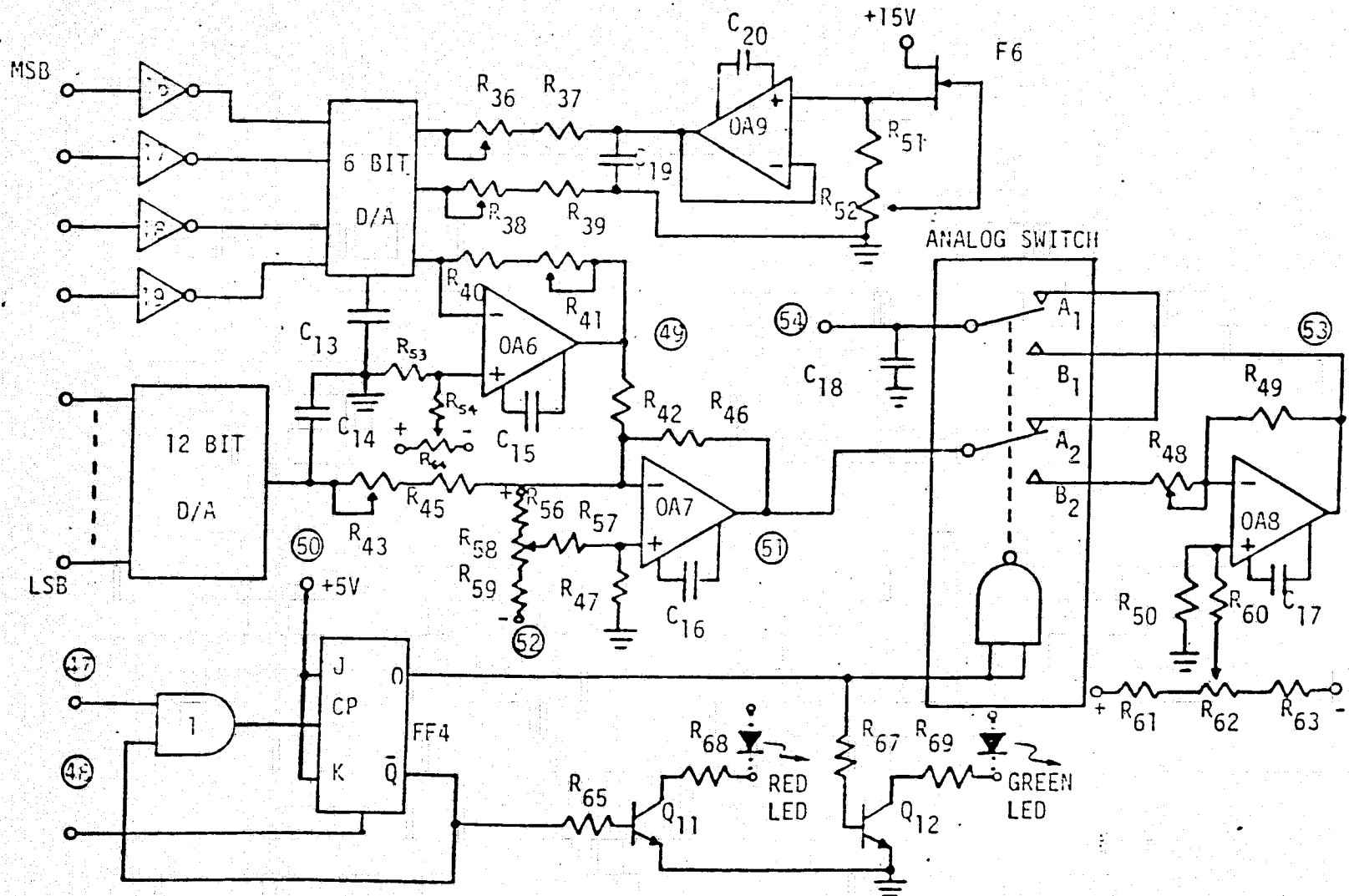


Figure 29. D/A Converter Circuit Diagram

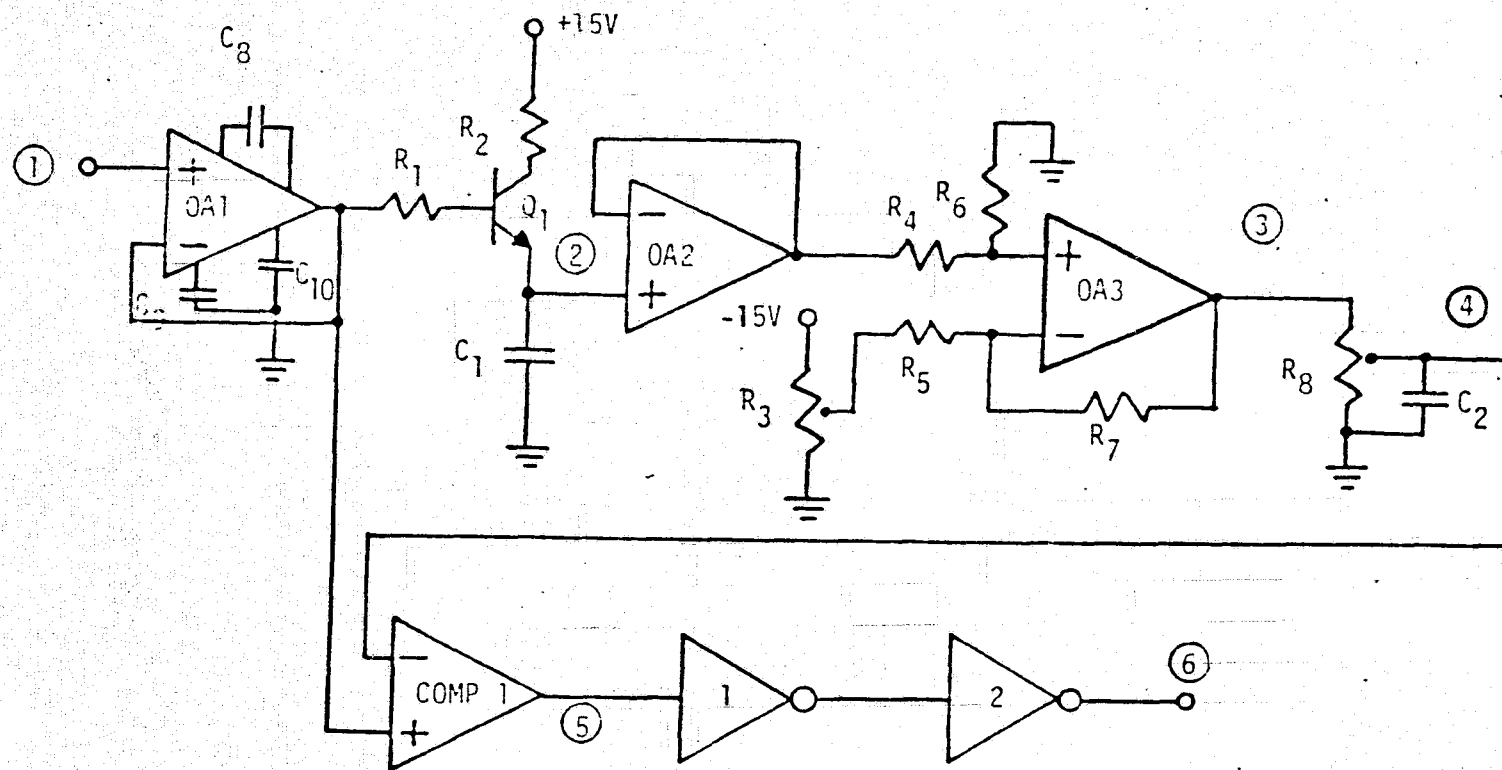


Figure 30. Pulse Amplitude Discriminator Circuit Diagram

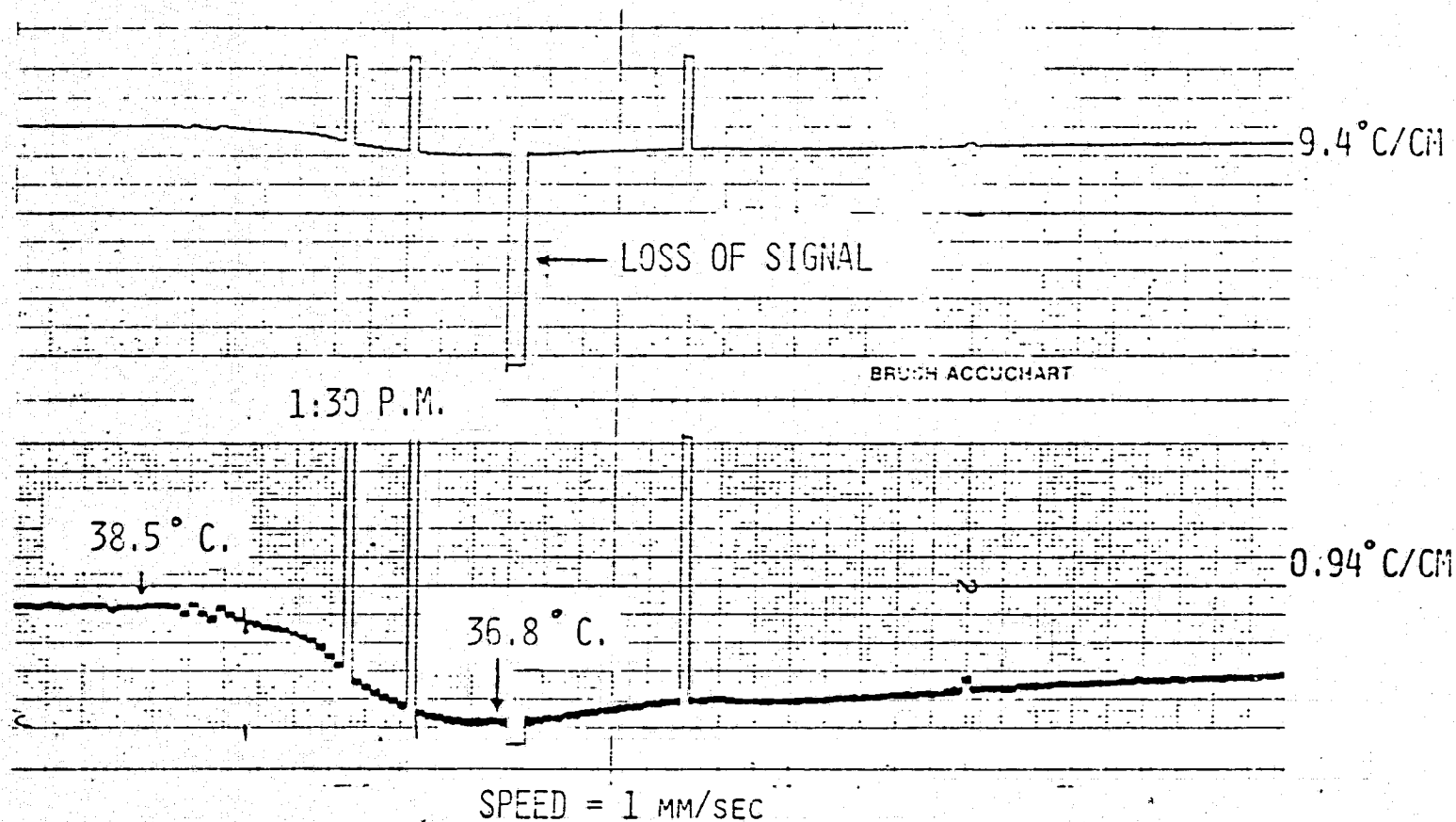


Figure 31. Strip Chart Recording Showing Temperature Response of Transmitter  
Inside the Dog's Intestinal Tract (Fluid Passing Transmitter)

#### D. M-5A PULSE FREQUENCY PFM MODULATOR

The main work done has been concentrated on the "M-5 Project." The goal of the project is to design and develop a Resistance-to-Pulse Frequency converted for application in implantable temperature biotelemetry. Specifications of the circuit were:

1. Operation from a single 1.3 volt battery.
2. Capability to produce low duty-cycle rectangular pulses with frequency controlled by a thermistor and stabilized (compensated) for battery voltage drift.
3. Suitability for integration in monolithic form using standard planar technology.
4. Capability to key a K-6 transmitter (20-100  $\mu$ A, >0.7 volt drive is required to turn the K-6 on).
5. Current consumption is less than 10  $\mu$ A on the average, with a duty cycle of  $10^{-2}$  or less.

The work done to achieve this goal can be summarized as follows:

1. Tests were performed on a previously designed and fabricated monolithic circuit (TS-1) to find out its failure in complying with the above requirements. It was concluded that the circuit design (M-5 circuit) was not compatible with the planar technology used which incorporates parasitic substrate transistors. An extensive report was written about the results of these tests (see Reference 1 or Reference 2).
2. As a solution, either the parasitic substrate transistor had to be eliminated by using a more sophisticated technology,

i.e. buried layer epitaxi, or a new circuit had to be developed which would not be degraded in performance by the parasitics involved. Considering the disadvantages of the circuit design of TS-1 chip (M-5), i.e. the use of temperature dependent and external compensation, the latter choice has been pursued.

3. In order to develop a new compensation method, a detailed study of the operation of complementary astable multivibrators was done. Based on the classification made, possibilities of compensation were investigated for each class of operation. The work concluded that Garg's method and the M-5 circuit were not the only possible methods, many new methods could be devised. (This work will be published soon.)

4. A new method called the "Positive- $V_T$  Method" was chosen to be best suited for integration in monolithic form. On a discrete model the method yielded less than 1.5% variation in frequency in a supply voltage range of 1.2 volts  $\leq V_{CC} \leq$  6.0 volts.

5. Based on the "Positive- $V_T$  Method" a monolithic RF converter was designed. The circuit was made multipurpose by incorporating a) a current differencer for increased sensitivity to resistance variation, and b) a differential V/I converter for voltage-to-pulse frequency conversion. The chip was named "M-5A". (Figures 32 and 33).

6. In the first two runs, poor contact and excessive leakage currents due to surface effects were encountered. The contact problem was eliminated by heating the wafers at 200°C during the aluminum metallization. The surface effects were eliminated by

minimizing contamination, using annealing steps which do not increase the oxide charge and using a forming gas treatment to decrease the surface recombination velocity.

7. In Class A-2 operation, the M-5A chip proved to be competitive to the hybrid M-7 circuit for ingestible temperature telemetry. It operated from a 1.3 volt battery with a total current drain as low as 1  $\mu$ A. The frequency is stable within 1% over a supply voltage range of 1.1 volt  $\leq V_{CC} \leq$  5.5 volts and the compensation is not effected by the thermistor resistance.

8. In Class B-2 and C-2 operations poor performance of a lateral P-N-P transistor at microampere level prevented attainment of compensation. Bulk recombination has been found to be responsible for this poor performance.

9. In spite of the poor P-N-P transistor gain ( $h_{FE} \approx 1$  at  $I_C \approx 1 \mu$ A) M-5A is an excellent V/F converter for ECG or EMG telemetry applications.

Differential input conversion gain = 2%/mV

$V_{CC} \geq 1.3$  volt

$I_{Total} \geq 5 \mu$ A (Can be decreased if P-N-P performance becomes better)

$R_{in} \approx 140$  K

CMMR  $\approx$  43 dB

when  $R = 330$  K  
 $V_{CC} = 1.3$  volt

$I_{Total} \approx 15$  A

10. Utilization of the chip in ECG telemetry has been shown.

A prototype optical ECG telemetry system was designed.

Transmitter:



$V_{CC} \approx 3.0$  volts

$I_{Total} = 7.0$  mA (40  $\mu$ A for M-5A, the rest for L.E.D.)

$f_C \approx 2$  KHz

Range: 5 cm

Reference 3 describes the unit.

11. Use of optical fiber coupling for increased range has been shown. The receiver section is being modified (redesigned) for better performance. The goal is:

Fiber Length  $\approx 1$  meter

Recent results imply feasibility of a system with:

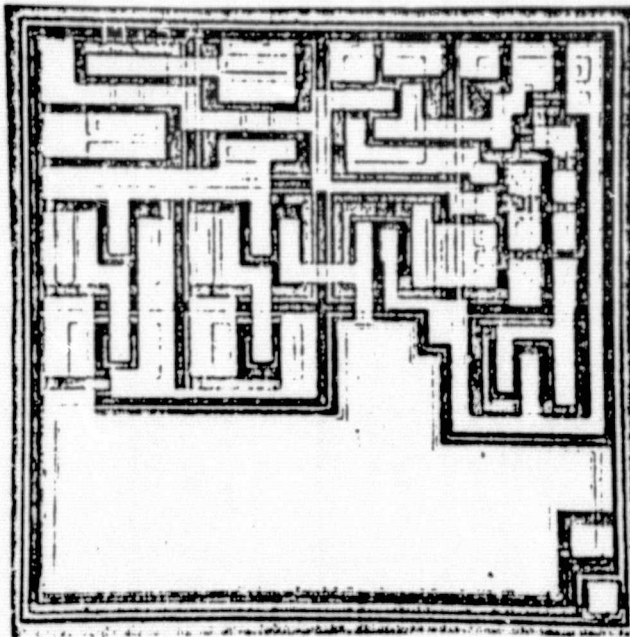
Transmitter Current  $\approx 50$   $\mu$ A, 2.8 volts

Net Voltage Gain  $\sim 10^4$

Fiber Length  $\sim 1 - 2$  meters

12. Efficiency of coupling of an infrared L.E.D. to a 20 mil diameter plastic fiber will be increased using a tapered guide.

- 
1. Guvenc, M.G., "Tests Performed on the TS-1 (M-5) Monolithic Circuit to Detect Problematic Points and Preliminary Proposals Toward Obtaining a Working Device" Report, (Memo No. 842), Microelectronics Lab., C.W.R.U., 1974.
  2. Guvenc, M.G., "A Monolithic Micropower Voltage and/or Resistance-to-Pulse Frequency Converter for Biomedical Telemetry Applications," Thesis (M.S.), School of Engineering, C.W.R.U., 1975.
  3. Guvenc, M.G., "An Optically Coupled ECG Telemetry System (M5A-OPTO-ACG)" Memo No. 847, Microelectronics Lab., C.W.R.U., 1974.



Dimensions:  $50 \times 50 \text{ mil}^2$

Epi: N-type,  $16\text{-}20\mu\text{m}$ , 2-4 ohm-cm

Substrate: P-type, 8 mils, 10-20 ohm-cm

Isolation Diffusion: Boron, 15 ohms/ $\square$ ,  $20\mu\text{m}$

Base Diffusion: Boron, 100 ohms/ $\square$ ,  $3.0\mu\text{m}$

Emitter Diffusion: Phosphorous, 4 ohms/ $\square$ ,  $2.0\mu\text{m}$

Figure 32. M-5A Monolithic Circuit Photograph and  
Fabrication Parameters

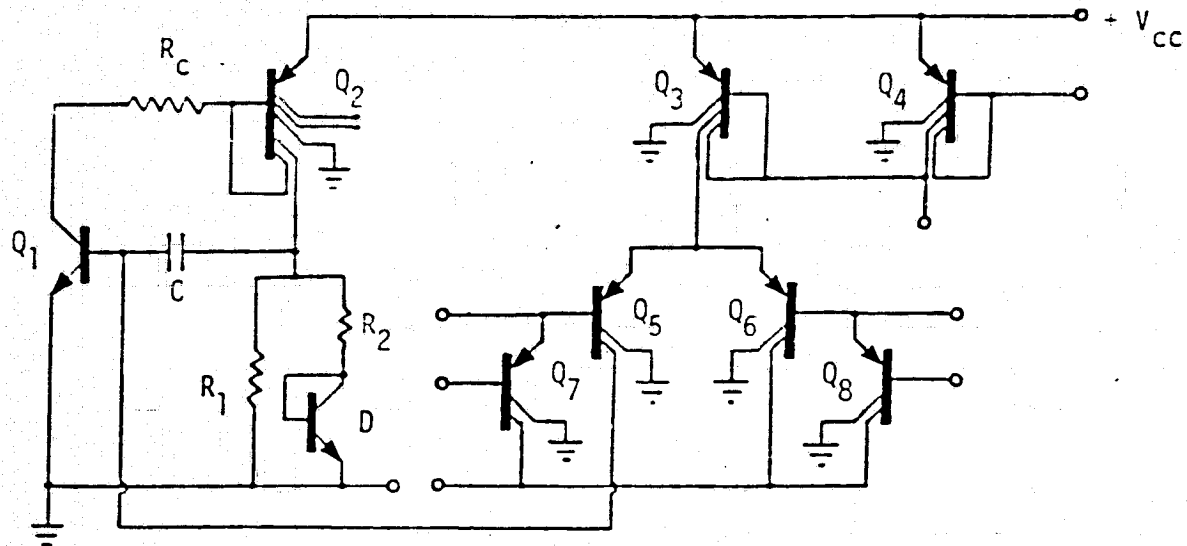


Figure 33. M-5A Circuit

## E. DEMODULATOR FOR THREE CHANNEL RF POWERED TELEMETRY SYSTEM

### Introduction:

In order to test the feasibility of the RF pulse powering for multichannel telemetry, a bench model of the three channel system was evaluated. Similarly, as in the single channel system, the transmitter in the three channel system is powered by an RF pulse burst and the signal information is received in between the powering pulses. The format of the entire multiplexed signal is shown in Figure 34. The transmitter has only one RF tank circuit which performs both receiving and transmitting functions. This approach not only saves the volume of the implant, but also eliminates possible cross coupling which results in systems where more than one RF frequency has to be used.

### Demodulator Description:

The signal format which is to be demodulated is shown in Figure 34.

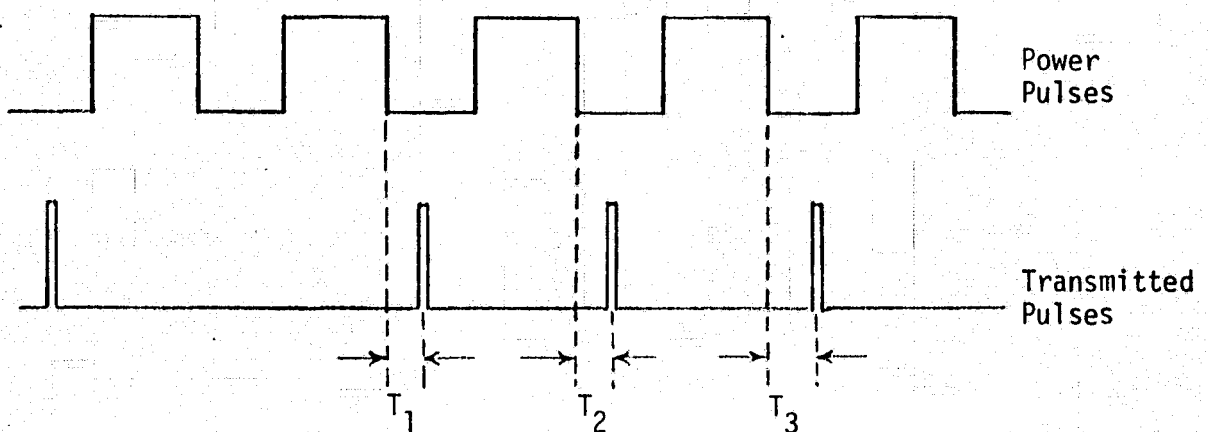


Figure 34. Signal Format

Multiplexing of the channels is sequential, and the transmitter is repowered after all channel information has been transmitted out. This

principle can be extended to virtually any number of channels with the only limitation being the maximum sampling rate. The proper synchronization for the demultiplexing was obtained by omitting one pulse in the transmitted train of pulses. This choice was considered for reasons of power consumption.

#### Demodulator Block Diagram:

The block diagram for the demodulator which is working with the signal format given in Figure 34, is given in Figure 35. The "antenna switch" circuit protects the input of the sensitive AM receiver during the RF powering pulse and is controlled by the antenna control pulse. The detailed circuit diagram is shown in Figure 36, and the function is self-explanatory.

The threshold detector detects the information pulse while filtering out the noise accompanying the received signal. Therefore, the error due to noise interference can practically be eliminated. This block also shifts the signal pulse level from  $0 \rightarrow +V_{CC}$  to  $\pm V_{CC}$  because the CMOS logic circuit which follows operates between  $\pm V_{CC}$ . A one-shot follows to provide the pulse width adjustment according to the sampling length requirement. The present width is set at  $12\mu\text{sec}$ . The circuit diagram is shown in Figure 37.

The ramp generator uses the stable Zener-diode voltage as a reference for the constant current supply source to charge the capacitor. The circuit is shown in Figure 38. From the circuit analysis, the ratio between the Zener's dynamic resistance ( $R_{dyn}$ ) and  $R_1$  (see Figure 38),  $R_1/R_X$  should, ideally, be as large as possible. This means that for each practical Zener, only one optimum operating point is available.

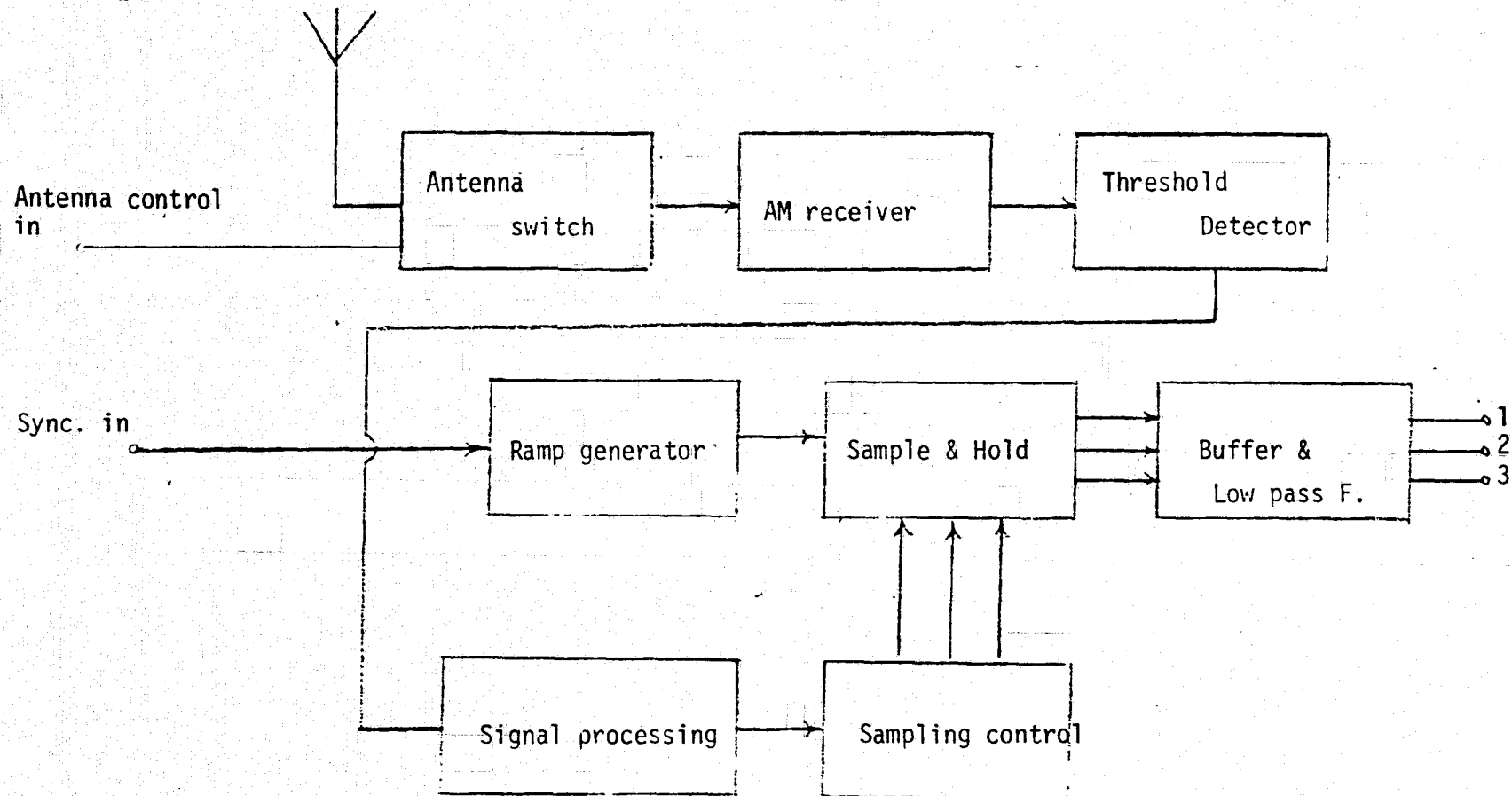


Figure 35. Demodulator Block Diagram

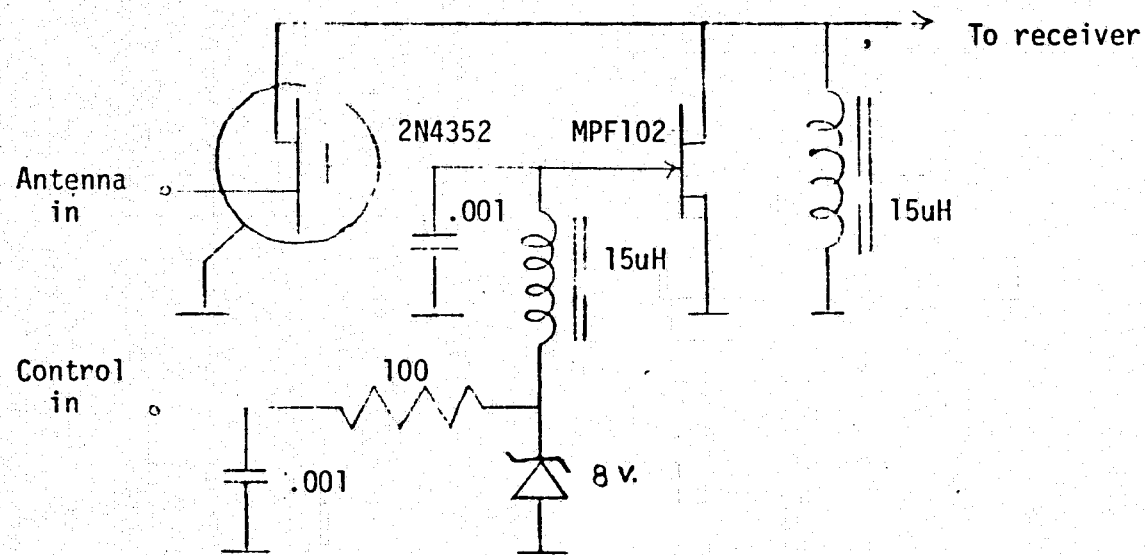


Figure 36. The Antenna Switch Circuit

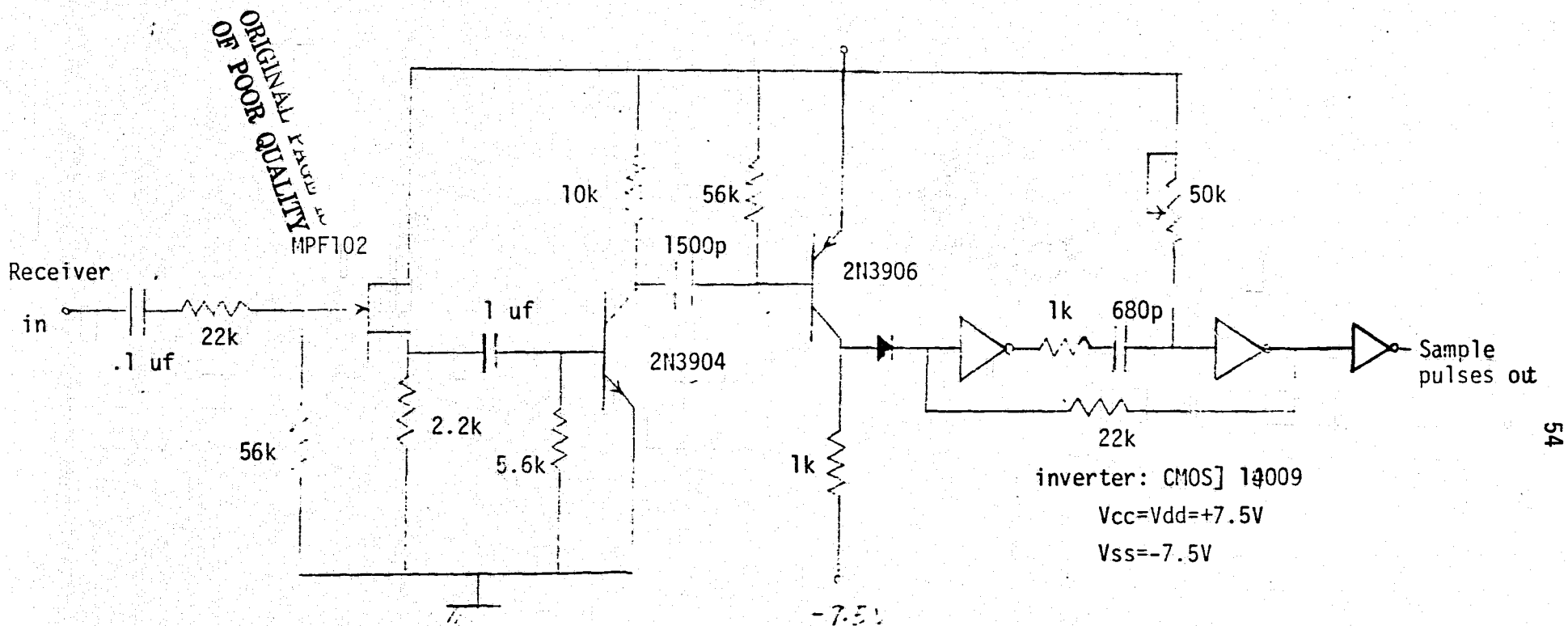


Figure 37. The Threshold Detector Circuit



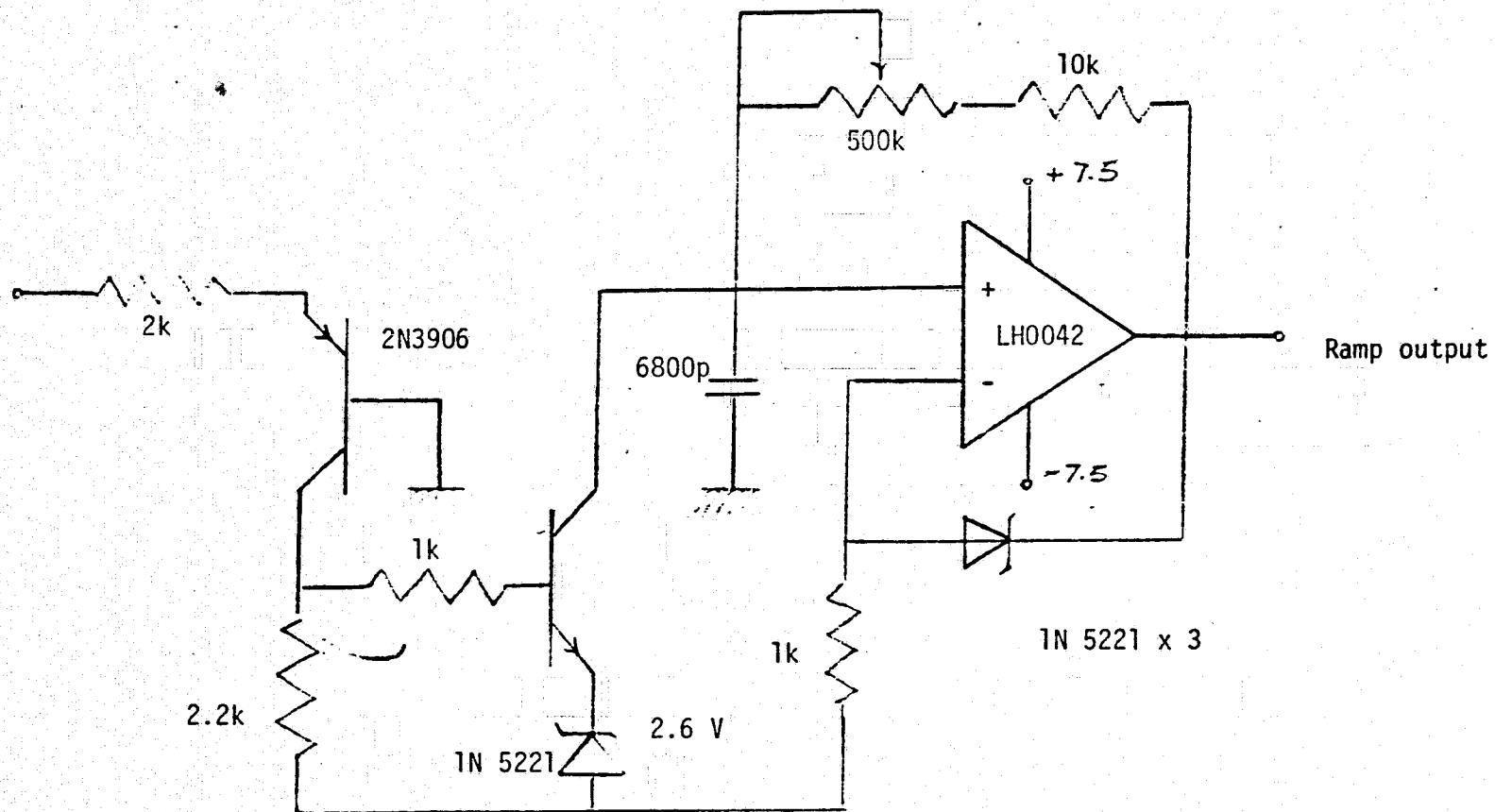


Figure 38. The Ramp Generator Circuit

The Zener presently used is a forward biased IN5221. Three in series gives about 1.5 volts and the  $R_1/R_{dyn}$  ratio is about 90. An LM103 regulator is intended to be used, since it gives very low  $R_{dyn}$  in the current range  $100 \mu A \rightarrow 10 \text{ mA}$ . Hence, a large  $R_1/R_{dyn}$  ratio can be obtained.

The signal processing unit demultiplexes the three channels. A CMOS logic is used here because of its high reliability and low power consumption. Since any signal in the RF powering period represents error, that period is blocked. The circuit diagram is shown in Figure 39. and the timing diagram is shown in Figure 40.

Sampling, holding and buffer stages are used for final signal processing. The circuit is shown in Figure 41. An analog gate was used for sampling, since its low on-resistance and excellent input-output delay time which were about  $400\Omega$  and 30 n-sec, respectively. The sampling time is 12  $\mu\text{sec}$ . The holding capacitance, 4,700p, gives a charging time constant of about 2  $\mu\text{sec}$ . An LH0042 operational amplifier was chosen for the buffer stage for its  $10^{12}\Omega$  input resistance and very low bias current.

#### Performance Summary:

Power supply:  $\pm 7.5$  volts, Raytheon RL4194 regulator

Supply Current: 26mA

Transmitting frequency: 65MHz

Sampling rate: 400/channel/sec.

Synchronization: 555 timer, 0 volt to  $+V_{CC}$  p - t - p.

1. 60 cycle noise: This is mainly due to the power supply ripple decoupling circuit which had been used for each circuit

board. The 60 cycle, seen at the output, is less than 5 mV.

2. Cross talk: With input of 5 V p - t - p sinusoid, the cross talk measured is about -60 dB, which is the typical CMOS multiplexer value.

3. Line coupling noise seen from the scope is about 15-20 mV, since it is measured after the low pass filter which had a high cut-off at 120 Hz. Probe pick up is of a high possibility.

4. Sensitivity:  $\Delta V_{out} / \Delta_{in} = 0.75$  (measured at transmitter power supply 7.5 volts).

5. Frequency response: Different input frequencies are applied and the output is recorded. According to the sampling theorem, with a sampling rate of 400/sec, it should be able to distinguish up to about 200 Hz signal. Since information content of interest is well beneath 100 Hz, frequency above 100 was ignored and was not put through the test. The attenuation of the higher frequency seen in the diagram was due to the frequency response of the chart recorder. The diagram is shown in Figure 42.

6. Sampling, holding drift is less than 4 mV.

7. The pulse position diagram and linearity test is shown in Figure 43.

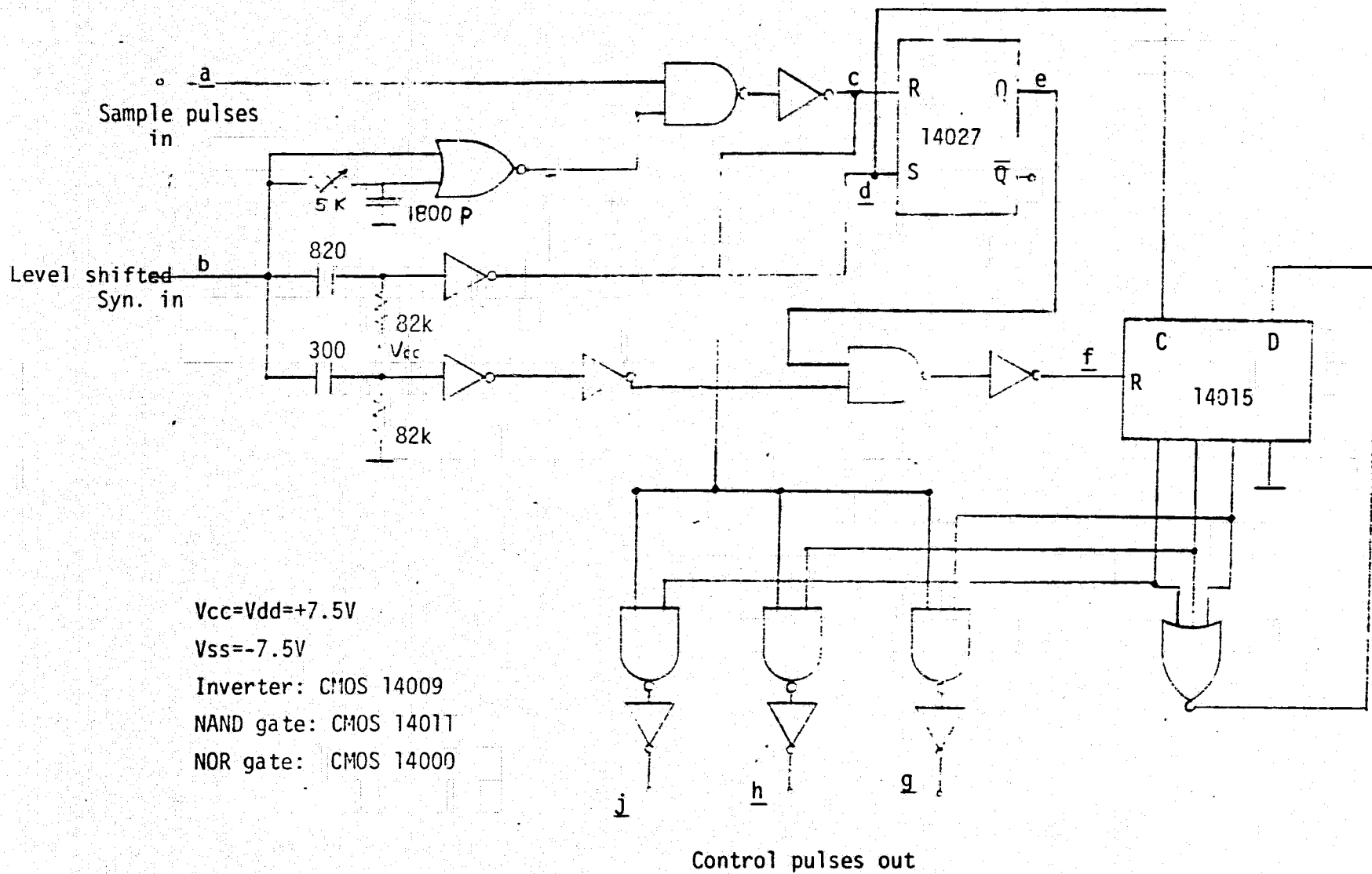


Figure 39. Signal Processing

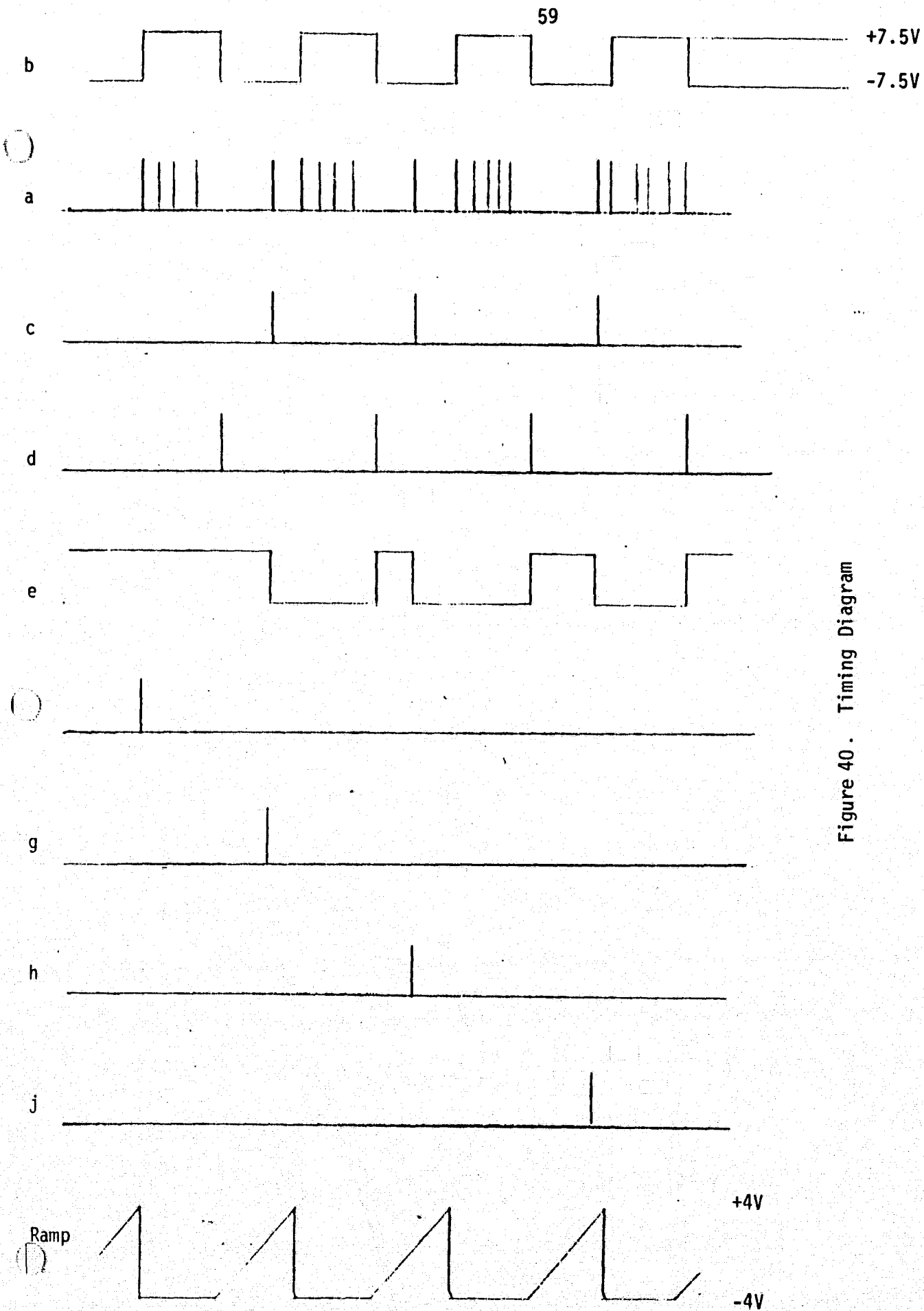


Figure 40 . Timing Diagram

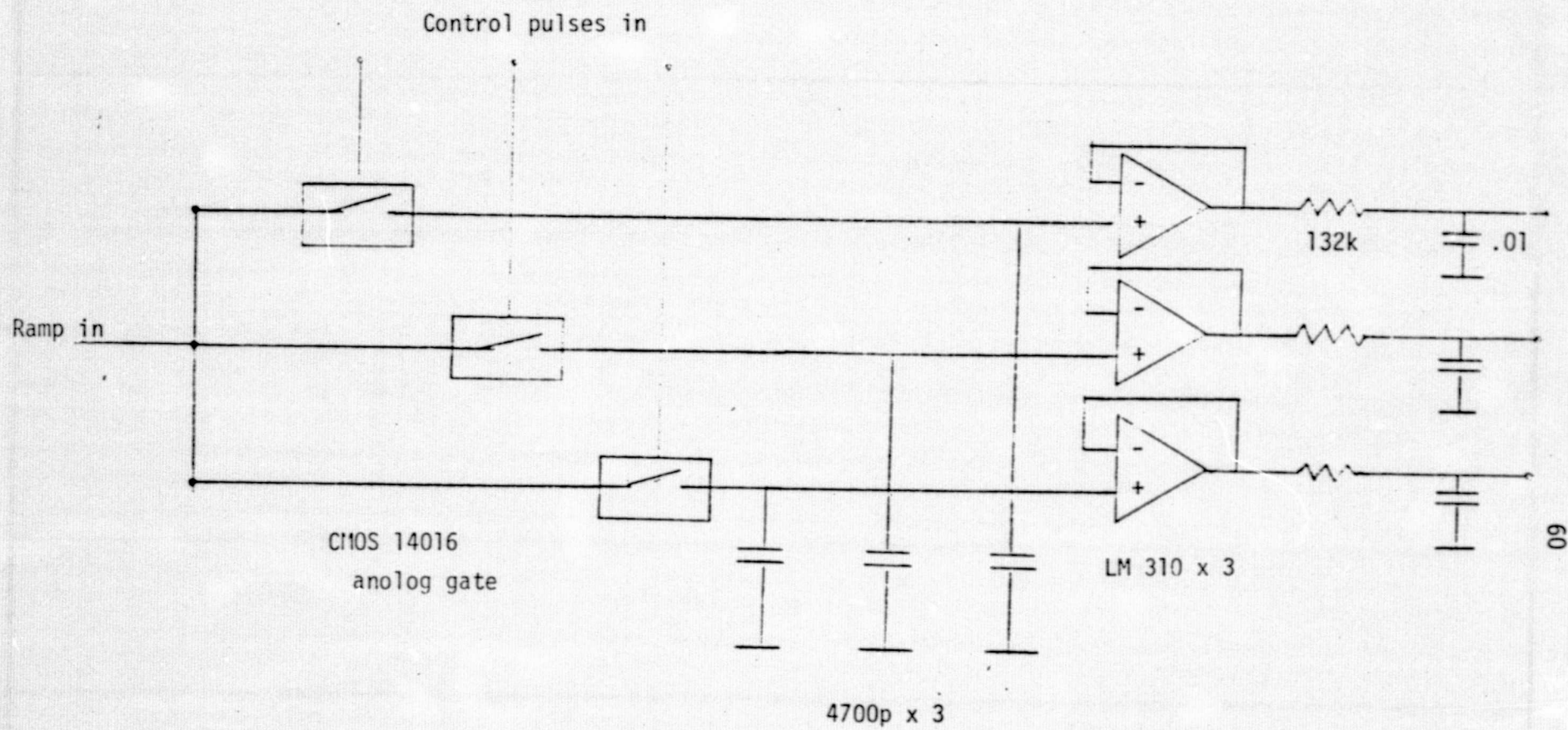
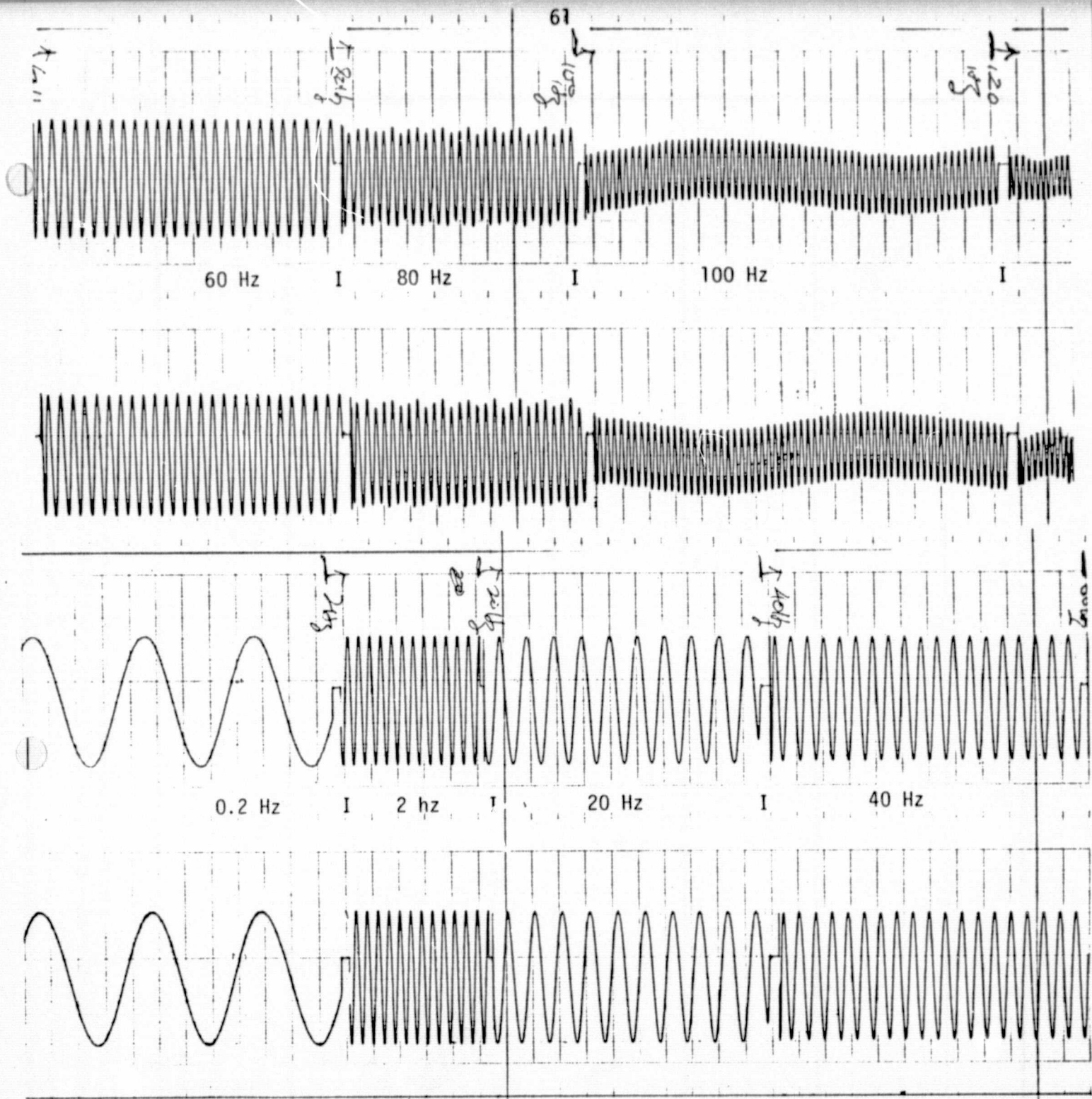


Figure 41. Sampling, Holding and Buffer Stage Circuit



ORIGINAL PAGE  
OF POOR QUALITY

Sensitivity of the chart: 200 mV/div.  
Sampling rate: 450/sec/channel

Figure 42. Output Record of Two Channels



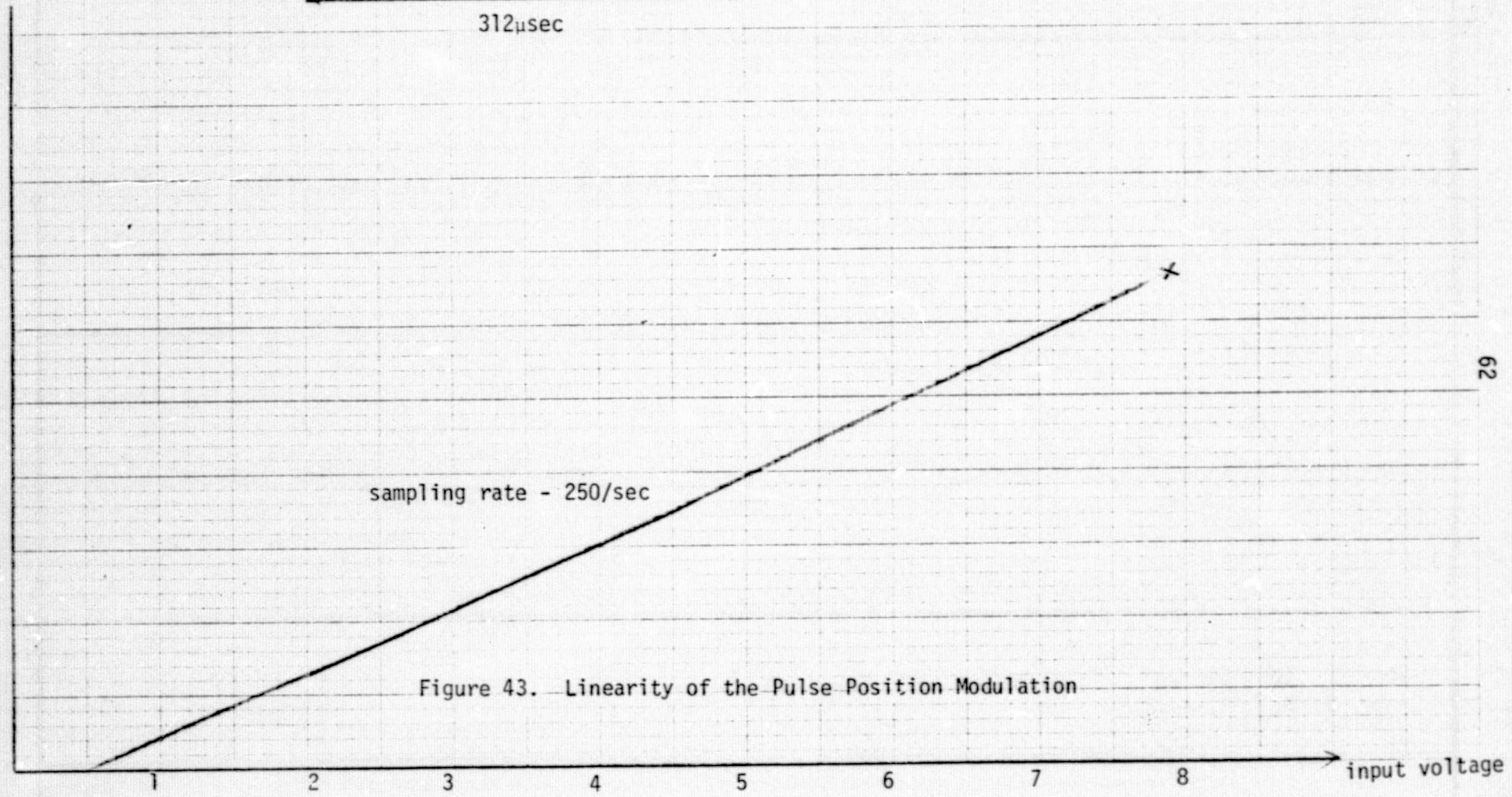
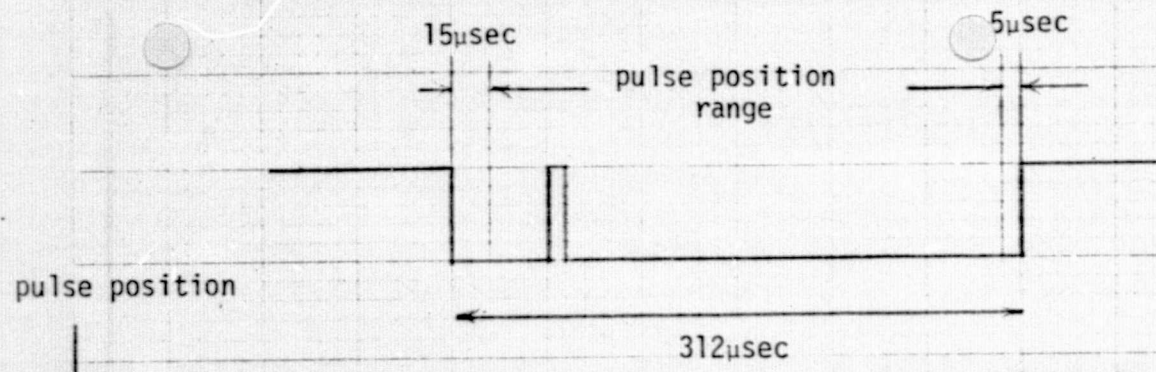


Figure 43. Linearity of the Pulse Position Modulation



The NASA Technical Officer for the grant is Thomas B. Fryer, NASA Electronic Instrument Development Branch, Ames Research Center, Moffett Field, California.

SECTION II  
PUBLICATIONS AND THESES

## A. JOURNAL ARTICLES AND PORTIONS OF BOOKS

1. "Telemetering of Biological Signals: Biotelemetry", W.H. Ko, in Handbook of Biochemistry and Biophysics, World Publishing Co., Cleveland, Ohio. pp. 636-643. 1966.
2. "A Six Channel Physiological Telemetry System", W.H. Ko with R. Robrock II. IEEE Trans. BME-14, No. 1: 40-46, January, 1967.
3. "Implant Biotelemetry and Microelectronics", W.H. Ko with M. Neuman. Science, Vol. 156, No. 3773: 351-360, April 21, 1967.
4. "A Study of Microwatt Power Pulsed Carrier Transmitter Circuits", W.H. Ko with W. C. Lin. Medical and Biological Engineering, Vol. 6: 309-317, 1968.
5. "Microelectronics, Bio-Instrumentation and Implants", W.H. Ko, pp. 375-402 in Bio-Engineering - An Engineering View, G. Bugliarello, Editor, San Francisco Press, 1968.
6. "Body Reaction of Implant Packaging Materials", W.H. Ko with M.R. Neuman and K.Y. Lin. Biomaterials, L. Stuart, Editor, Vol. 10, Plenum Press, New York, 1968.
7. "Biotelemetry", W. H. Ko, in Biomedical Engineering Systems, Vol. 10. M. Clynes and J.H. Melsun, Editors, McGraw-Hill, New York, 1970.
8. "Fast Charging Circuit for NiCd Battery Used in Implant Electronic Systems", W.H. Ko with W. Lin and O. Agrawal. IEE Trans. on BME-17, No. 4: 331-334, October, 1970.
9. "Taped-On Heart Rate and ECG Telemetry Transmitters", W.H. Ko with E.T. Yon, S. Mabrouk and J. Hyncek. J. Assn. for Advancement of Med. Instrumentation, Vol. 5, No. 5: 268-272, September, 1971.
10. "Microelectronics and Miniaturization", W.H. Ko, Chapter 70 in Medical Engineering, Yearbook Medical Publishers, Inc., Chicago, Illinois, 1974.
11. "Radiation from an Electrically Small Circular Wire Loop Implanted in a Dissipative Homogeneous Spherical Medium", W.H. Ko with R. Plonsey and S.R. Kang. Annals of Biomedical Engineering, 1, No. 2: 135-146, December, 1972.
12. "Radiation from an Electrically Small Off-Centered Loop in a Dissipative Homogeneous Spherical Medium", W.H. Ko with S.R. Kang, Annals of Biomedical Engineering, Vol. 2, pp. 321-325, 1974.

## B. CONFERENCE PAPERS

1. "Miniature FM Implant Biotelemetry Transmitters" and "RF Induction Power Supply for Implant Circuits". W.H. Ko. 6th International Conference on Medical Electronics and Biological Engineering, Tokyo, Japan, August 20-25, 1965.
2. "An Implant Telemetry System for the Measurement of Internal Strain". W.H. Ko. 18th Conference on Engineering in Medicine and Biology. Philadelphia, Pennsylvania, November, 10-12, 1965.
3. "An Implantable System for the Myoelectric Stimulation of Skeletal Muscle Using RF Links", W.H. Ko with R. Lorig, L. Vodovnik, et.al. Proc. 1967 Conference on Engineering in Medicine and Biology, Section 28.6, 1967.
4. "Implantable Multiple-Channel Telemetry System of Biomedical Research", W.H. Ko with W. Thompson, E. Yon. 1968 IEEE National Telemetry Conference, Houston, Texas, April, 1968.
5. "Experimental Study of Packaging Materials for Microelectronic Implants", W.H. Ko with F. Critchfield, K.Y. Lin and M. Neuman. 21st Annual Conf. on Engineering in Medicine and Biology, Houston, Texas, November, 1968.
6. "A Real Time Electrocardiogram Waveform Identifier", W.H. Ko with K. Morgan, W. Lin and J. Liebman. 21st Annual Conference on Engineering in Medicine and Biology, Houston, Texas, November, 1968.
7. "An Intravaginal Fetal ECG Telemetry System", W.H. Ko with M. Neuman, F. Critchfield and W.C. Lin. 21st Annual Conference on Engineering in Medicine and Biology, Houston, Texas, November, 1968.
8. "An Implantable Pulsed Microwatt Power Transmitter Circuit Insensitive to Battery Voltage Variation", W.H. Ko with W. Lin, B. Garg and O. Agrawal. 21st Annual Conf. on Engineering in Medicine and Biology, Houston, Texas, November, 1968.
9. "Taped-On Heart Rate and ECG Telemetry Transmitters", W.H. Ko with E.T. Yon. 5th Annual Association for the Advancement of Medical Instrumentation, Boston, Mass., March. 1970.
10. "Micropower Pulse Modulated Telemetry Transmitter", W.H. Ko with E.T. Yon and J. Hyncek. 23rd Annual Conference on Engineering in Medicine and Biology, Washington, D.C. November, 1970.
11. "A Multiple Channel Monolithic Integrated Circuit Biomedical Telemetry System", W.H. Ko with D. Ramseth and E.T. Yon. 23rd ACEMB, Washington, D.C., November, 1970.

12. "Micropower Pulse Modulated Multiplex Telemetry System", W.H. Ko 9th International Conference on Medical and Biological Engineering, Melbourne, Australia, August, 1971.
13. "A General Purpose Micropower Monolithic Telemetry System", W.H. Ko with D. Conrad, E. Yon and J. Hynecek. 9th ICMBE, Melbourne, Australia, August, 1971.
14. "A Monolithic Biomedical Pressure Sensor Utilizing the Piezo-resistive Effect", W.H. Ko with E. Blaser and E. Yon. 9th ICMBE, Melbourne, Australia, August, 1971.
15. "Micropower Two-Channel Telemetry System for EKG and Temperature Signals", W.H. Ko with W.C. Lin and S. Pillay. 9th ICMBE, Melbourne, Australia, August, 1971.
16. "A Miniature Digital Pressure Transducer", W.H. Ko with E.M. Blaser and E.T. Yon. 24th Annual Conference on Engineering in Medicine and Biology, Las Vegas, Nevada, November, 1971.
17. "Development of Dual Channel Telemetry System for Perinatal Monitoring", W.H. Ko with E. Yon, M. Neuman, J. Hynecek and A. Zeewy, 26th ACEMB, Minneapolis, Minnesota, October, 1973.
18. "Implant Telemetry for Intracranial Pressure Monitoring," W.H. Ko with E. M. Cheng, R.J. Lorig and B.H. Clague, 27th ACEMB, Philadelphia, Pennsylvania, October, 1974.
19. "Single Frequency RF Powered Telemetry System", W.H. Ko with J. Hynecek, 28th ACEMB, New Orleans, Louisiana, September, 1975.
20. "A Micropower Modulator Chip for Temperature and Biopotential Telemetry", W.H. Ko with M.G. Guvenc, 28th ACEMB, New Orleans, Louisiana, September, 1975.
21. "Fiber Optics Coupled Pulse-Frequency Modulated ECG Telemetry System", W.H. Ko with M.G. Guvenc, 28th ACEMB, New Orleans, Louisiana, September, 1975.

## AN INGESTIBLE TEMPERATURE TELEMETRY SYSTEM

Abstract by Chie Wan Poon

An ingestible temperature telemetry system based on the existing M-3 temperature telemetry system<sup>(17)</sup> was redesigned. The system can also be used in subcutaneous implantation and other body cavities for temperature monitoring.

The transmitter redesigns include the following:

1. Lower power drain to extend the lifetime of the battery to six months or more.
2. Wider operating temperature range ( $0^{\circ}\text{C}$  -  $60^{\circ}\text{C}$ ).
3. Linearity of better than  $\pm 0.1^{\circ}\text{C}$  in a  $+5^{\circ}\text{C}$  range at  $37^{\circ}\text{C}$ .

Methods of packaging and encapsulation were explored and reported.

The receiving system was also redesigned with up-to-date electronic integrated circuits to give better performance in the noise discrimination schemes. The output format was also improved for convenient reading.

System performance was evaluated on an ingestion experiment with a normal dog. The results and future suggestions are given subsequently.

THE CONTROL AND DEMODULATION SYSTEM FOR A SINGLE CHANNEL  
RF POWERED IMPLANTABLE TELEMETRY TRANSMITTER

Abstract by Steven Gerald Todd

The control and demodulation system for a single channel RF powered implantable telemetry transmitter was designed, built and tested.

The telemetry transmitter uses a single L-C tuning tank, to minimize the implantation size, for both the RF power absorption and the telemetry transmission. Pulse delay modulation is used to encode the electrocardiogram (ECG) data using the trailing edge of the RF power up burst envelope as the reference for the delay before the telemetry burst. The RF power transmission and the telemetry transmission are at a fixed frequency between forty and sixty megacycles.

The control and demodulation system was built to prove the feasibility of a small externally RF powered telemetry transmitter. Secondly, the system was designed and built to anticipate the difficulties that might be encountered in similar, but more sophisticated systems operating on the same system principles of small implant size with an external RF power source.

The control system generates the RF power used by the implantable telemetry transmitter and controls the timing and sequence of the power up period and the telemetry period. The demodulation system uses synchronization from the control circuit and pulse information from the telemetry receiver to decode the ECG information from the

implant circuit. The ECG information is sampled and transmitted every 34 milliseconds in the prototype system for a maximum theoretical information bandwidth according to the Nyquist sampling theorem of  $1/2T$ , or 150 cps.

The resultant capability of this system is that it be able to monitor ECG information with a minimum of risk and discomfort to the implant host for whatever period of time is required.